The origin and evolution of wide Jupiter Mass Binary Objects in young stellar clusters

Simon F. Portegies Zwart,
Erwan Hochart

Leiden Observatory, Leiden University, PO Box 9513, 2300 RA, Leiden, The Netherlands
* spz@strw.leidenuniv.nl

Abstract

The recently observed population of 540 free-floating Jupiter-mass objects, including 40 dynamically soft pairs, and 2 triples, in the Trapezium cluster has raised interesting questions on their formation and further evolution. We test various scenarios for the origin and survivability of these free floating Jupiter-mass objects and Jupiter-mass Binary Objects (JuMBOs) in the Trapezium cluster. The numerical calculations are performed by direct N-body integration of the stars and planets in the Trapezium cluster starting with a wide variety of planets in various configurations. We discuss four main models: $\mathcal{SPP}$ in which selected stars have two outer orbiting Jupiter-mass planets; $\mathcal{SPM}$ where selected stars are orbited by Jupiter-mass planet-moon pairs; $\mathcal{ISF}$ in which JuMBOs form in situ together with the stars, and $\mathcal{FFC}$ where we introduce a population of free floating single Jupiter-mass objects, but no binaries. Models $\mathcal{FFC}$ and $\mathcal{SPP}$ spectacularly fail to produce enough JuMBOs. Models $\mathcal{SPM}$ can produce sufficient free floaters and JuMBOs but require to start with unusually wide orbits for the planet-moon system around the star. The observed populations of JuMBOs and free floating Jupiter-mass objects in the Trapezium cluster are best reproduced if they formed in pairs and as free floaters together with the other stars in a smooth (Plummer) density profile with a virial radius of ~ 0.5 pc. A fractal (with fractal dimension 1.6) stellar density distribution works also, but requires them to have formed relatively recently ($\lesssim 0.3$ Myr ago), with a high ($\gtrsim 50\%$) initial binary fraction. This would make the primordial binary fraction of jumbos even higher than the already high observed fraction of ~ 8 % (42/540). The fraction of JuMBOs will continue to drop with time, and the lack of jumbos in Upper Scorpius could then result of its higher age, causing more JuMBOs to be ionized. We then also predict that the interstellar density of Jupiter-mass objects (either single or some, $\sim 2\%$, lucky surviving binaries) is ~ 0.05 JuMBOs per pc^{-3} (or around 0.24 per star).

1 Introduction

Recently [1] reported the discovery of 42 Jupiter-Mass Binary Objects (JuMBOs) in the direction of the Trapezium cluster. Their component masses range between 0.6 $M_{\rm Jup}$ and 14 $M_{\rm Jup}$ and they have projected separations between 25 au and 380 au. Two of these objects have a nearby tertiary Jupiter-mass companion. They also observed a population of 540 single objects in the same mass range. This discovery initiates the discussions on the origin and surviveability of weakly bound Jupiter-mass pairs in a clustered environment.

The first single free-floating Jupiter-mass objects have been found in the direction of the Trapzium cluster more than 20 years ago [2–4]. Many more have been found since then, for example in the young clustered environment of Upper Scorpius [5], and through gravitational microlensing surveys in the direction of the Galactic bulge [6]. Their abundance may be as high as $1.9^{+1.3}_{-0.8}$ per

star [6], although a considerable fraction of these could be in wide orbits around a parent star, or have masses $\ll M_{\rm Jup}$.

The origin of these free floating planets has been actively debated [7]. Star formation, from the collapse of a molecular cloud through gravitational instability, generally is expected to lead to objects considerably more massive than Jupiter [8,9], and in disks planets tend to form with lower masses. As a consequence, the large population of Jupiter-mass free-floaters is often considered to result from fully packed planetary systems [10], or kicked out of their orbit by encounters with other stars in the young cluster [11]. Single Jupiter-mass free floating objects then originally formed in a disk around a star to become single later in time [11–16]. But [17] argue that single jupiter-mass objects could form in star forming regions. The number of super-Jupiter mass free floating objects formed in this way is expected to be on the order of one (~ 0.71) per star [11], but lower-mass free floaters orphaned this way may be much more abundant [14]; The origin of relatively massive free-floaters through dynamical phenomena is further complicated by the tendency for lower mass planets to be more prone to ejections [16, 18–20].

Explaining the observed abundance and mass-function of single free-floating Jupiter-mass objects is difficult. In particular the large population of objects in Upper Scorpius challenges the formation channels. The new discovery of a large population of paired free-floaters complicates matters even further, and puts strong constraints about their origin. So far, binary free-floating planet-mass object have been rare, and were only discovered in tight (few au) orbits [21], including:

- 2MASS J11193254-1137466 AB: a 5 to 10 $M_{\rm Jup}$ primary in a $a = 3.6 \pm 0.9$ au orbit [22].
- WISE 1828+2650: a 3 to 6$M_{\rm Jup}$ primary with a 5 $M_{\rm Jup}$ companion in an $\gtrsim 0.5$ au orbit [23].
- WISE J0336-014: a 8.5 to 18 $M_{\rm Jup}$ primary with a 5 to 11.5 $M_{\rm Jup}$ companion in a $0.9^{+0.05}_{-0.09}$ au orbit [24].
- 2MASS J0013-1143 discovered by [25] and suspected to be a binary by [26].

Such tight pairs could have formed as binary planets (or planet-moon pairs) orbiting a stars, to be dislodged from their parents to become JuMBOs [27]. So long only a few were discovered such an exotic scenario seems to pose a reasonable explanation for their existence, but the discovery of a rich population of 42 wide JuMBOs [1] requires a more thorough study on their origin.

Adopting a dynamical origin, or at least a dynamical history, we perform direct N-body simulations of a Trapezium-like star cluster with primordial Jupiter-mass objects (JMO) and JuMBOs. Our simulations focus on four models that could explain the abundance, their masses, and the orbital characteristics (actually the observed separation distribution) of the observed Jupiter-mass objects in the cluster. Alternative to forming in situ (scenario $\mathcal{ISF}$), one can naively imagine three mechanisms to form JuMBOs. [28] argued that these binaries could be explained from hierarchical planetary systems of which the outer two planets are stripped by a passing star in a close encounter. The two ejected planets would lead to a population of free floating planets, but could also explain the observed population of JuMBOs. We call this scenario $\mathcal{SPP}$ (for star planet-planet).

Alternatively one could imagine JuMBOs to result from planet-moon pairs (or binary planets) orbiting some star that is ejected to become a JuMBO. We call this scenario $\mathcal{SPM}$, for star planet-moon. Finally, we explore the hypothesis of how a sufficiently large population of free-floating Jupiter-mass objects could lead to a population of JuMBOs by dynamical capture of one JMO by another. We call this scenario $\mathcal{FFC}$ (free floating capture). A similar scenario was proposed by [29] for explaining very wide stellar pairs, but the model was also adopted to account for wide planetary orbits [30, 31]

We start by discussing some fundamental properties of the environmental dynamics in section 2, followed by a description of models in section 3, the numerical simulations to characterize

the parameters of the acquired JuMBOs in section 4, and the resulting occurrence rates in section 5. We conclude in section 6.

2 The dynamical characterization of JuMBOs

The JuMBOs discovered by [1] were located in the Trapezium cluster. We base our analysis on the parameters derived for this cluster by [32] who numerically modelled of disk-size distributions observed in the Trapezium cluster, and concluded that this distribution is best reproduced for a cluster containing ~ 2500 stars with a total mass of $\sim 900\,M_\odot$ and a half-mass radius of ~ 0.5 pc. The results were inconsistent with a Plummer [33] distribution, but match the observations if the initial cluster density distribution represented a fractal dimension of 1.6 (see [34]). Nevertheless, for consistency with earlier studies, we perform our analysis for Plummer as well as for a fractal distributions (with fractal dimension 1.6).

Adopting a Plummer distribution of the Trapezium cluster (with virial radius $r_{\rm vir} = 0.5$ pc), the cluster core radius $r_c \simeq 0.64 r_{\rm vir} \sim 0.32$ pc with a core mass of $250\,M_\odot$, resulting in a velocity dispersion of $v_{\rm disp} \equiv GM/(r_c^2 + r_{\rm vir}^2)^{1/2} \simeq 0.97$ km/s. With a mean stellar mass in the cluster core of $1\,M_\odot$ the unit of energy expressed in the kinematic temperature kT becomes $\sim 8 \cdot 10^{42}$ erg.

Jumbos are found in the mass range of about $0.6\,M_{\rm Jup}$ to $14\,M_{\rm Jup}$ and have a projected separation of 25 au to 380 au. The averaged observed values are $d = 200 \pm 109$ au, $\langle M \rangle = 4.73 \pm 3.48\,M_{\rm Jup}$, and $\langle m \rangle = 2.81 \pm 2.29\,M_{\rm Jup}$. The median and 25 % to 75 % percentiles are $r_{ij} = 193.8^{+78.2}_{-114.1}$ au $M = 3.67^{+1.31}_{-1.57}\,M_{\rm Jup}$, and $m = 2.10^{+1.05}_{-1.05}\,M_{\rm Jup}$ which we calculated from the data in table 1 of [1].

To simplify our analysis, let us assume that the observed variation in projected distances between the two Jupiter-mass objects corresponds to an orbital separation, and express distances in terms of semi-major axis (see Appendix A for motivation). In practice, the differences between the projected separation and the actual semi-major axis of the orbit is small. Adopting a statistical approach, a thermal distribution in eccentricities and a random projection on the sky, the semi-major axis is statitically ~ 1.2 times the projected separation. For the observed JuMBOs we do not really know if they are bound, and if so, we do not know the underlying eccentricity distribution, but in practice this difference between projected separation and actual semi-major axis of a bound population is negligible compared to the 25% to 75% uncertainty intervals derived from the simulations.

To first order, the binding energy of jumbos then ranges between $\sim 5 \cdot 10^{37}$ erg and $1.4 \cdot 10^{41}$ erg, or at most ~ 0.02 kT. This makes them soft upon an encounter with a cluster star. The hardest JuMBO, composed of two $14\,M_{\rm Jup}$ planets in a 25 au orbit would be hard for another encountering object of less then $17\,M_{\rm Jupiter}$. For an encountering $1\,M_{\rm Jup}$ object a 25 au orbit would be hard only if the two planets are about three times as massive a Jupiter. This entails that JuMBOs are generally soft for any encountering free floating giant planet unless they are in tight enough orbits or the perturber is of low mass. On average, soft encounters tend to soften these binaries even further [35], although an occasional soft encounter with another planet may actually slightly harden the JuMBO. Independent of how tight the orbit, JuMBOs are expected to be relatively short lived, because they easily dissociate upon a close encounter with any other cluster member. The JuMBO ionization rate is then determined by the encounter probability, rather than the encounter parameters.

Once ionized they contribute to the population of free floating single objects. Note that in the Trapezium cluster, even the orbits of 2MASS J11193254-1137466AB, and WISE 1828+2650 would be soft ($\gtrsim 0.025$ kT); they could be the hardest survivors of an underlying population.

To further understand the dynamics of JuMBOs in a clustered environment, and to study the efficiency of the various formation scenarios we perform direct N-body calculations of the

Trapezium star cluster with a population of Jupiter-mass objects in various initial configurations.

3 Model calculations

For each of our proposed models, $\mathcal{ISF}$ (in situ formation of jumbos), $\mathcal{SPP}$ (JuMBOs formed via ejections of a host stars outer planets), $\mathcal{SPM}$ (as planet-moon pairs orbiting a star), and $\mathcal{FFC}$ (mutual capture of free-floaters) we perform a series of N-body simulations with properties consistent with the Trapezium cluster.

Each cluster starts with 2500 single stars taken from a broken power-law mass-function [36] between 0.08 $M_\odot$ and 30 $M_\odot$ distributed either in a Plummer sphere (model Pl) or a fractal distribution with a fractal dimension of 1.6 (model Fr). All models start in virial equilibrium. We run three models for each set of initial conditions, with a virial radius of 0.25 pc, 0.5 pc and 1.0 pc, called model R025, R05 and R100, respectively. We further assume stellar radii to follow the zero-age main sequence, and the radius of Jupiter-mass objects based on a density consistent with Jupiter ($\sim$ 1.3 g/cc).

For each of our proposed models, we initialize a population of single JMOs and/or JuMBOs (binary JMOs). The single (and the primaries in planet pairs) are selected from a power-law mass function between 0.8 $M_{\rm Jup}$ and 14 $M_{\rm Jup}$, which is consistent with the observed mass function [1]. We fitted a power-law to the primary-planet mass function, which has a slope of $\alpha_{\rm JuMBO} = -1.2$ (considearbly flatter than Salpter's $\alpha_{\rm Salpter} = -2.35$).

This relatively flat mass function is consistent with the mass distribution of earlier observed free floaters The first dozen discovered free floaters already seemd to have a rather flat mass function [3], but the large statistics available through gravitational microlensing surveys allowd a reliable measure of the slope, which yields $\alpha = -1.3^{+0.3}_{-0.4}$ [6]. This mass function is somewhat steeper than the slope derived for lower-mass ($\lesssim 1\ M_{\rm Jup}$) free floaters ($\alpha = -0.96^{+0.47}_{-0.27}$ [37]).

For each of the four models, we have a special set of initial configurations. The clusters all have the same statistical representation, being either Plummer or fractal density distributions, virialized and with a virial radius of 0.25 pc, 0.5 pc, and 1.0 pc. But the distribution of JMOs and JuMBOs varies per model. In figure 1 we scetsch the various models.

3.1 Model $\mathcal{FFC}$: Jupiter-mass objects as free-floating among the stars

For the models with free-floating Jupiter-mass objects, model $\mathcal{FFC}$, we sprinkle the single objects from a power-law distribution with a slope of $\alpha = -1.2$ in the cluster potential as single objects using the same initial distribution function as we used for the single stars (either Plummer or fractal). These models were run with $\sim$ 600 objects with a mass $> 0.8\,M_{\rm Jup}$. Most runs are performed with 600 JMOs.

We performed additional runs with 10^4 free floaters. Some of These runs have a different lower-limit to the mass function, to keep the number of objects with a mass $> 0.8\,M_{\rm Jup}$ at $\sim$ 600 (assuming that objects of lower-mass objects are unobservable). Each simulation is evolved for 1 Myr, after which we study the population of free floating Jupiter-mass objects and the population of JuMBOs. A few simulations were extended to 10 Myr, to study the long term surviveability of JuMBOs.

3.2 Model $\mathcal{SPP}$: Star hierarchically orbited by two planets

For scenario $\mathcal{SPP}$, we selected the star to host a planetary system from the 150 stars lower in mass than 0.6 $M_\odot$ and 150 more massive stars. The mid-mass point (of 0.6 $M_\odot$) is almost twice the mean stellar mass in the mass function.

The mass of the primary planet, $M_{\rm prim}$, was chosen from the same power as used for model section 3.1. The mass of the secondary planet, $M_{\rm sec}$, was selected randomly from a thermal distribution between $0.2M_{\rm prim}$ and $M_{\rm prim}$. The more massive planet can then either be the inner planet or the outer one. A consequence of our mass-ratio distribution is that we have a slight preference for planets of comparable mass, and that we have a population of $\lesssim 0.8\,M_{\rm Jup}$ objects, which were not observed. This low-mass population contributes to $\sim 7.3\,\%$ of the total.

The distance from the first planet a_1 and the second planet a_2 (such that $a_2 > a_1$) are selected according to various criteria. The inner orbit a_1 was selected randomly between 25 au and 400 au from a flat distribution in a. The outer orbit, a_2, was typically chosen to be five times larger than the inner planet's Hill radius. This guarantees that the planetary systems would be stable when in isolation.

Both planetary orbits are rather circular with a random eccentricity from the thermal distribution between circular and 0.02. The two planets orbit the star in a plane with a relative inclination randomly between -1° and 1°. The other orbital elements are randomly taken from their isotripic distributions. Also the orientation of the system in space was randomized. We perform an additional series of simulations with pre-specified orbital separations for the two planets a_1 and a_2, to follow the model proposed in [28]. The results of these runs are presented in figure 11 in section 5.1.

3.3 Model $\mathcal{SPM}$: Star orbited by a pair of planet-mass objects

In the $\mathcal{SPM}$ models we initialize planet pairs (or planet-moon pair) in orbit around a star. The masses of the stars, planets and moons are selected as in the $\mathcal{SPP}$ model. The planet-moon system's orbit was selected from a flat distribution in a between 25 au and 200 au, and with a eccentricity from the thermal distribution with a maximum of 0.02.

To warrant stability of the star-planet-moon system, we choose an orbital separation such that the planet-moon pair stays within 1/3th of it's Hill radius in orbit around the star. The eccentricity of the system is smaller than 0.02 taken randomly from the thermal distribution. The planet-moon system is randomly orientation. These systems tend to be dynamically stable, but some fraction may be subject to von Zeipel-Lidov-Kozai cycles [38–40]. With the adopted range of masses and orbital parameters the time-scale for a cycle is of the order of a few Myr. Two Jupiter-mass objects in a circular 100 au orbit around a 1 $M_\odot$ star would lead to a circum-stellar orbit of $\sim$ 3490 au. von Zeipel-Lidov-Kozai cyle period of such a system $\lesssim 1.6$ Myr, depending on the eccentricity of the planet-moon system around the star.

3.4 Model $\mathcal{ISF}$: Jupiter-mass objects in weakly bound orbits

Primordial JuMBOs (model $\mathcal{ISF}$) are initialized with semi-major axis with a flat distribution between 25 au and 1000 au, an eccentricity from the thermal distribution between 0 and 1, but they are to remain separated at pericenter. The masses are selected as in model $\mathcal{SPP}$. Each system is subsequenlty rotated to a random orientation. The binaries are sprinkled in the cluster potential as single objects using the same initial distribution function as used for the stars.

In figure 1 we illustrate the four models with a schematic diagram.

3.5 The simulations

All calculations are performed using 4-th order prediction-correction direct N-body integrator PH4 [41] through the Astrophysical MUltipurpose Software Environment, or AMUSE for short [42–44]. The data files are stored in AMUSE formatted particle sets, and available via zenodo `10.5281/zenodo.10149241`; the source code is available at github `https://github.com/spzwart/JuMBOs`.

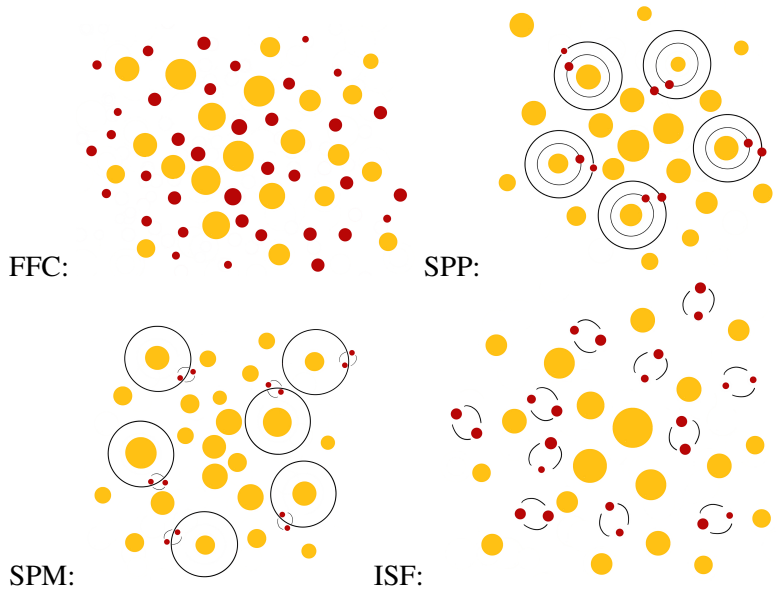

Figure 1: Illustration of the four configurations for Jupiter-mass planets in the stellar cluster. Stars are represented with yellow bullets, and planets in red. From top left to bottom right we have (as indicated): model $\mathcal{FFC}$ for the free floating single planets; $\mathcal{SPP}$ for outer orbiting planets; $\mathcal{SPM}$ as bound planet-moon pair orbiting a star, and model $\mathcal{ISF}$ in situ formation of jumbos.

The script to run the simulations is fairly simple. It is essentially the same script from chapter 2 in [44], including the collision-detection stopping condition. Runs are performed with the default time-step parameter $\eta = 0.03$, which typically leads to a relative energy error $< 10^{-8}$ per step, and $\lesssim 10^{-5}$ at the end of the run. The fractal initial conditions with small virial radius (0.25 pc) are, not surprisingly, the hardest runs to perform. The energy error in these runs can be somewhat higher at times, but never exceed $< 10^{-3}$, which according to [45], suffices for a statistically reliable result. Snapshots were stored every 0.1 Myr, and the simulations were continued until 1.1 Myr, but we analyse the data at an age of 1 Myr.

Although incorporating stellar evolution, general relativity and the Galactic tidal field would be straightforward in the AMUSE framework, we decided to ignore those processes. We do not expect any stars to effectively lose much mass during the short duration of the simulations. Incorporating general relativity would have made the calculations expensive without much astrophysical gain, and the tidal field has hardly any influence on the close encounter dynamics in the cluster central portion. On the other hand, in the observations, JuMBOs seem to be confined towards to the cluster central region. This, however, is in part an observational selection effects, as it is difficuly to identify Jupiter-mass objects away from the cluster center due to intercluster extinction and the lower coverage at the periphery (S. Pearson, private communication).

3.6 Finding JuMBOs

JuMBOs are soft in terms of the average local kinetic energy of the surrounding objects (stars and planets), and this makes them somewhat hard to find in the numerical models. One generally consider hard binary paris or multiples in direct N-body simulations and finding those soft pairs requires some extra effort. We search for JuMBOs by first selecting any object in the cluster, star or planet, find the nearest neighbors, and determine their binding energy. If one of these companions has another object as bound nearests neighbor, we adopt that as the close pair, and the initially selected object as the tertiary. Later, we order the particles in terms of distance and

binding energy, on which the eventual designation is based.

Instead of identifying JuMBOs as bound pairs, we also analyse the data with just the nearest neighbors using connected components. With this method we do not establish JuMBOs as bound objects, but as close pairs. This second method is to mimic the observations, in which boundness cannot yet be established.

We recognize single stars s, and planets p (although we are uncertain weather or not to call these objects planets). Pairs of objects are then placed in parenthesis, for binary stars we write (s, s), a planetary system with one planet can be (s, p). A system with two planets then either becomes $((s, p), p)$, for a hierarcy of planets, or $(s, (p, p))$ for a planet pair orbiting a star as in the $\mathcal{SPM}$ model. A JuMBO in this nomenclature becomes (p, p).

4 Results

The main results of the calculations are presented in table 1 and table 2, but also in the more fine-tuned simulations presented in table 3.

The large parameter space of how to distribute JMO's among stars, we start by covering part of this space with a selection of simulations in which we vary the way JMOs and JuMBOs are distributed among the stars. In addition, we cover a small portion of the cluster parameter space, including the virial radius and the density profile. All the other parameters we keep constant.

The results of these simulations are reported in section 4.1, and in the tables 1 and 2 in section 4.4.

In section 4.5 we further explore our favorite model in which JuMBO form as isolated pairs together with the stars.

4.1 Distinghuising between the various models

In table 1 we list per model the number of different outcomes. The various simulation results are named after their model designation followed by either the letter "Pl" for the Plummer model, or "Fr" for the Fractal model. The model name ends with the virial radius "R" in parsec, here R025 indicates 0.25 pc, R050 for 0.5 pc and R100 for 1 pc virial radius.

The $\mathcal{SPP}$ and $\mathcal{FFC}$ models systematically fail to reproduce the observed population of JuMBOs by a factor of 50 to 400. Changing the initial distribution in semi-major axis of the inner orbit from a uniform distribution to a logarithmic distribution reduces the formation rate of JuMBOs even further. There are several systematic trends in terms of cluster density and Plummer versus fractal distribution, but it is not clear how these models can lead to JuMBOs. Both models produce a considearble population of binary stars and single planetary systems, in particular in the fractal distributions, where the typical fraction of dynamically formed binary stars is around 4 %, and the fraction of JMO's captured by a star is 0.7 % per star. Interestingly, the model that already start with some paired configuration with a star tends to produce more binaries and planetary systems, that the models where planet-mass objects do not orbit stars. The high abunance of hierarchical multiple planets, $((s, p), p)$, in the $\mathcal{SPP}$_Pl and $\mathcal{SPM}$_Pl models reflects some of the initial conditions. These models also tend to produce a relatively rich population of single planet systems (s, p).

The only models that produce a considerably population of JuMBOs are the $\mathcal{SPM}$ models and the $\mathcal{ISF}$. Where for the latter the Plummer distributions tend to produce sufficient number of JuMBOs whereas the fractal model produce too few.

Rather than directly investigating the orbital separattions, in figure 2 we present the distribution of nearest mutual distance between stars and JMOs for model $\mathcal{ISF}$_Fr_R050. Model $\mathcal{ISF}$_Pl_R050 shows similar trends, but less pronounced. Note there for calculating the nearest

Table 1: The average number of systems per simulations model categorized in groups. The possible outcomes are the number of single stars (n_s), binaries ($n_{(s,s)}$), star orbited by a single planet ($n_{(s,p)}$), star orbted by two planets ($n_{((s,p),p))}$), single isolated planets (n_p) and JuMBOs ($n_{(p,p)}$). Note that we only list those objects with a mass $> 0.8\,M_{\rm Jup}$. As a consequence, the total number of planary mass objects does not always add up to 600. The number of stars also does not always adds up to 2500 because of collisions and hierarchies not listed in the table (see section 4.2).

model	n_s	$n_{(s,s)}$	$n_{(s,p)}$	$n_{((s,p),p))}$	n_p	$n_{(p,p)}$
$\mathcal{FFC}$_Pl_R025	2271	87	11	0	580	0
$\mathcal{FFC}$_Pl_R050	2313	83	3	0	595	0
$\mathcal{FFC}$_Pl_R100	2331	75	5	0	593	0
$\mathcal{FFC}$_Fr_R025	2280	93	11	0	584	0
$\mathcal{FFC}$_Fr_R050	2336	74	4	0	592	0
$\mathcal{FFC}$_Fr_R100	2312	85	5	0	594	0
$\mathcal{SPP}$_Pl_R025	2287	0	84	129	258	0
$\mathcal{SPP}$_Pl_R050	2224	1	42	232	93	0
$\mathcal{SPP}$_Pl_R100	2204	0	19	277	26	0
$\mathcal{SPP}$_Fr_R025	2308	72	8	0	591	0
$\mathcal{SPP}$_Fr_R050	2279	83	28	6	560	0
$\mathcal{SPP}$_Fr_R100	2327	64	27	10	553	0
$\mathcal{SPM}$_Pl_R025	2480	0	17	3	413	18
$\mathcal{SPM}$_Pl_R050	2457	0	36	7	341	44
$\mathcal{SPM}$_Pl_R100	2464	0	22	14	394	15
$\mathcal{SPM}$_Fr_R025	2320	76	1	0	448	5
$\mathcal{SPM}$_Fr_R050	2293	90	2	0	444	17
$\mathcal{SPM}$_Fr_R100	2361	61	3	0	447	26
$\mathcal{ISF}$_Pl_R025	2498	0	0	0	425	23
$\mathcal{ISF}$_Pl_R050	2498	1	0	0	362	48
$\mathcal{ISF}$_Pl_R100	2500	0	0	0	246	108
$\mathcal{ISF}$_Fr_R025	2334	53	7	0	392	0
$\mathcal{ISF}$_Fr_R050	2309	81	7	0	450	4
$\mathcal{ISF}$_Fr_R100	2345	73	0	1	454	6

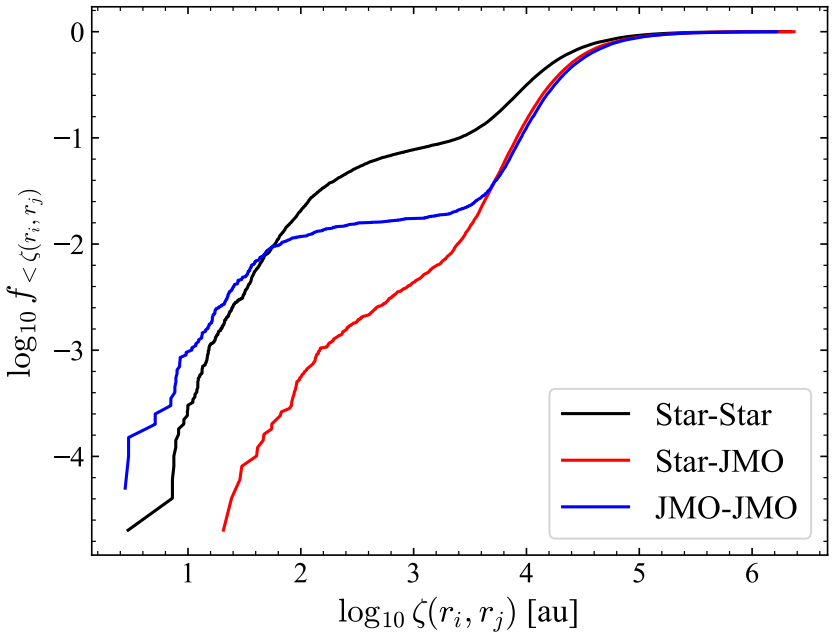

Figure 2: Mutual nearest neighbor distribution function for model $\mathcal{ISF}$_Fr_R050. Each object star or JMO is treated as separate, and then we establish distributions for the mutual nearest neighbor distance for pairs of stars, pairs of JMOs and for the distance between a star and a JMO. **ERWAN: This is the best figure in the paper. Could you make a version with added dotted lines for the Plummer model R050?**

mutual distance we treated all JuMBOs as two separate JMO. This gives rise to the left shoulder in the blue curve in figure 2. This shoulder is also visible in the star-star curve (black), at a higher elevation above $\sim$ 100 au, but below a few tens of au JMO-JMO pairs are relatively more abundant. The distribution for the mutual distance between stars and JMOs does not show such a pronoundced shoulder, and for distances $r_{ij} \gtrsim 10^4$ au both distributions converge.

Having established the existence of an overpopulation of nearest neigbors among stars and JMOs, we further explore the orbital characteristics of the surviving JuMBOs. The median, the 25% and 75% quartiles for the JuMBO, (p, p), distribution for primary mass, secondary mass, semi-major axis and eccentricity are presented in table 2. The models that produce too few JuMBOs to calculate the median and quartiles are omitted. We adopt the medial values with the quarlites as realiable interval for comparing the observational data with the simulations because the distributions are rather skewed. This is noticeable in the large difference between the sizes of the lower and the upper quartiles.

The primary masses produced in the models $\mathcal{SPM}$ and $\mathcal{ISF}$, tend to be on the high side, but the secondary masses are in the observed range. All the $\mathcal{SPM}$ models tend to lead to orbits that are too tight, but omitting the orbits with $a < 25$ au JuMBOs does not improve the median orbital separation. In terms of the orbital separation (or projected distance) the best model seems to be $\mathcal{ISF}$ Plummer with a 0.5 pc virial radius, but the distributions are wide, and although the 1 pc $\mathcal{ISF}$ fractal model exhibits a low formation rate, it does reproduce the observed separation distribution. Note that models $\mathcal{ISF}$_Fr at an age of 0.2 or 0.3 Myr compare quite fovarably to the observations (see section 5).

The eccentricities in model $\mathcal{SPM}$_Pl are generally smaller than in the fractal models. The planet-moon pairs in those models started in almost circular orbits. In the fractal models, the eccentricities are more effectively perturbed and thermalized, whereas in the Plummer models this does not happen. In model $\mathcal{ISF}$, JuMBOs start with higher average eccentricities, in which case

Table 2: Simulation results for the models that produce a sufficiently large population of JuMBOs to be considered feasable (mainly models $\mathcal{SPM}$ and $\mathcal{ISF}$). We present the median values and the quartile intervales for 25 % and 75 %. The observed median inter-JMO distance in the Trapezium cluster is $r_{ij} = 193.8^{+78.2}_{-114.1}$ au $M_{\rm prim} = 3.67^{+1.31}_{-1.57}\,M_{\rm Jup}$, and $M_{\rm sec} = 2.10^{+1.05}_{-1.05}\,M_{\rm Jup}$ [1].

model	$\langle M\rangle/M_{\rm Jup}$	$\langle m\rangle/M_{\rm Jup}$	$\langle a\rangle$/au	$\langle e\rangle$
$\mathcal{SPM}$_Pl_R025	$3.62^{+1.36}_{-2.68}$	$1.12^{+0.24}_{-2.14}$	$99.08^{+37.24}_{-36.38}$	$0.47^{+0.18}_{-0.13}$
$\mathcal{SPM}$_Pl_R050	$4.02^{+2.10}_{-3.71}$	$1.74^{+0.73}_{-0.93}$	$94.28^{+32.78}_{-78.90}$	$0.33^{+0.19}_{-0.27}$
$\mathcal{SPM}$_Pl_R100	$6.93^{+4.38}_{-3.07}$	$1.29^{+0.23}_{-1.22}$	$140.96^{+37.10}_{-11.20}$	$0.12^{+0.05}_{-0.27}$
$\mathcal{SPM}$_Fr_R025	$2.66^{+1.78}_{-3.20}$	$1.87^{+1.05}_{-0.37}$	$35.56^{+20.57}_{-62.84}$	$0.80^{+0.10}_{-0.18}$
$\mathcal{SPM}$_Fr_R050	$9.64^{+7.02}_{-1.99}$	$2.00^{+0.69}_{-0.58}$	$82.76^{+21.74}_{-83.04}$	$0.56^{+0.29}_{-0.18}$
$\mathcal{SPM}$_Fr_R100	$4.60^{+2.57}_{-2.44}$	$1.80^{+0.64}_{-2.47}$	$73.20^{+27.21}_{-100.43}$	$0.38^{+0.21}_{-0.13}$
$\mathcal{ISF}$_Pr_R025	$8.12^{+3.44}_{-4.51}$	$2.10^{+0.98}_{-1.66}$	$112.06^{+40.76}_{-181.76}$	$0.43^{+0.08}_{-0.19}$
$\mathcal{ISF}$_Pl_R050	$7.00^{+3.28}_{-4.23}$	$2.03^{+0.68}_{-0.99}$	$296.40^{+168.53}_{-190.04}$	$0.62^{+0.19}_{-0.12}$
$\mathcal{ISF}$_Pl_R100	$5.25^{+2.37}_{-3.16}$	$1.60^{+0.72}_{-1.40}$	$457.63^{+265.29}_{-193.56}$	$0.67^{+0.23}_{-0.14}$
$\mathcal{ISF}$_Fr_R050	$4.82^{+3.05}_{-4.42}$	$1.38^{+0.75}_{-2.42}$	$37.57^{+15.07}_{-42.46}$	$0.77^{+0.06}_{-0.05}$
$\mathcal{ISF}$_Fr_R100	$10.15^{+3.75}_{-2.84}$	$1.98^{+0.50}_{-2.13}$	$97.05^{+47.34}_{-189.07}$	$0.77^{+0.17}_{-0.16}$

de difference in eccentricity between the Plummer and fractal models is less pronounced. Later, in section 4.5, we will explore $\mathcal{ISF}$ models with initially curcular orbits.

4.2 Stellar and planetary collisions

We encountered quite a number of collisions in the simulation, but the majority occur between two stars (83%), with the rest between a star and a Jupiter-mass object. Collisions between two Jupiter-mass objects are very rare. Most collisions happen in the fractal models. In figure 3 we present the cumulative distribution of collisions in the models ISF_Fr with a virial radius of 0.25 pc (solid blue), 0.5 pc (orange) and 1.0 pc (green), and for the equivalent models FFC_Pl with the thin dash-dotted curves. The higher density naturally leads to more collisions, and those collisions tend to occur earlier in time.

Plummer models tend to lead to fewer collisions. The only Plummer models in which collisions among stars were common is in model $\mathcal{FFC}$ with 64, 20 and 18 collisions on average per cluster, for those models with a viral radius of 0.25 pc, 0.5 pc and 1.0 pc, respectively. Interestingly enough, the fractal models from the same series only experience 30, 17 and 14 collisions for the same virial radii. It came as a bit of a surprise that models $\mathcal{FFC}$_Pl lead to so many collisions, even though no collisions happen between two Jupiter-mass objects.

4.3 Runaway JuMBOs

In addition to mergers, ejection events also occurred. We adopt the classical definition of identifying runaway objects if their velocity with respect to the center of mass of the entire stellar system (dominated by the bound cluster) exceeds 30 km/s [46].

Not surprisingly, no JuMBO escaped the cluster with a high velocity, but there are some slow runaways, which were born in the cluster periphery and never experienced an encounter with a nearby star. Adding a tidal field to our calculations may cause this population to increase.

Single runaway stars and JMOs are also rare in our simulations. We attribute this rareness to the lack of hard binaries in the initial conditions. We encounter on average one runaway JMO for each of the fractal models, and typically twice as many runaway stars. The JMOs, however have on average a velocity of 110 km/s, whereas the stars escape with $\sim$ 63.3 km/s.

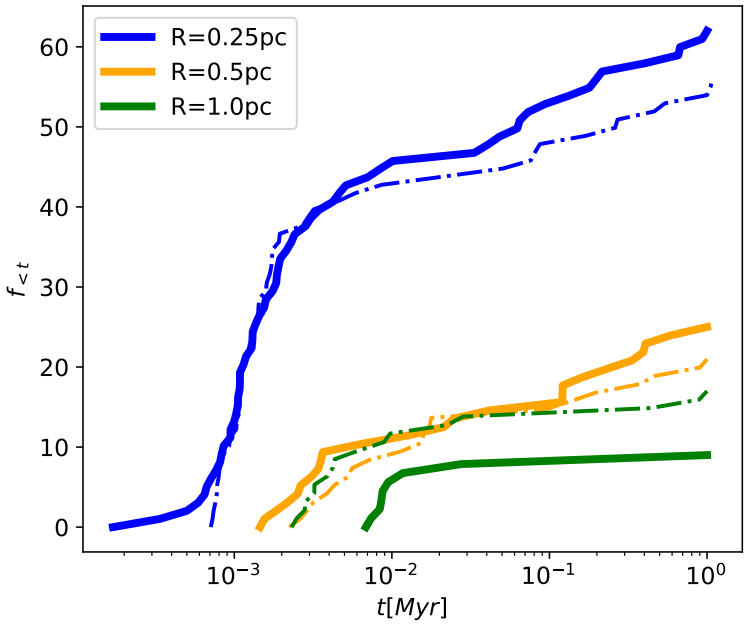

Figure 3: Number of collisions as a function of time for model $\mathcal{SPM}\_Fr$ (solid lines) and for models $\mathcal{FFC}\_Pl$ (dash-dotted lines).

4.4 Fine-tuning for the binary fraction and separation distribution

Having established that we prefer model $\mathcal{ISF}$, we will further explore the consdequences, and try to derive some of the earlier JuMBO properties to see if those are reconcilable with our understanding of planet and star-formation in section 4.5.

In figure 4 we illustrate how the fraction of jumbos rapidly decreases with time in models $\mathcal{ISF}$_Pl_R050 and $\mathcal{ISF}$_Pl_R100 (and the equivalent fractal models) for the light blue and red curves. The binary fraction among jupite-mass objects initially drops quickly (even exponentially in the fractal models), to slow down after $\sim$ 0.2 Myr at a survival fraction of $\sim$ 2 % for the 0.5 pc virial radius and $\sim$ 10 % for the 1 pc virial radius cluster. For the latter model, the fraction of JuMBOs drops eventually to about 4 %; lower than the observed 8 %.

To investigate the evolution of the mean orbital separation of the surviving JuMBOs, and the effect of changing the initial distribution in orbital separation, we present figure 5. Here we show how the distribution in orbital separation of the jumbos in model $\mathcal{ISF}$_Pl_R050 rapidly drops with time, and converges in $\lesssim$ 0.1 Myr to a median separation < 100 au. This distribution is much narroware and on average with a smaller mean than observed in the Trapezium cluster.

We further explore the effect of changing the initial eccentricity or semi-major axis distribution, but these choices do not seem to make a sufficienly big difference to salvage the fractal models for explaining the observed population of JuMBOs. Starting with a tighter population of JuMBOs will help delaying their ionization, but hardly affects the eventual distribution in orbital separation. On the other hand, it will help in making the fraction of JuMBOs consitent with the observations. Such consistency is reached $\sim$ 0.2 Myr or 0.3 Myr after the start of the simulations. At this time, the fraction of JuMBOs to JMOs as well as the separation distribution of the surviving JuMBOs are consistent with the observed population. We consider this a strong argument in favor of JuMBOs as late formed objects.

In figure 6 we present the orbital distribution for JuMBOs in model $\mathcal{ISF}$_Fr050 (with and without free floating JMOs) at a age of 0.2 Myr. Shortly after the JuMBOs are introduced in

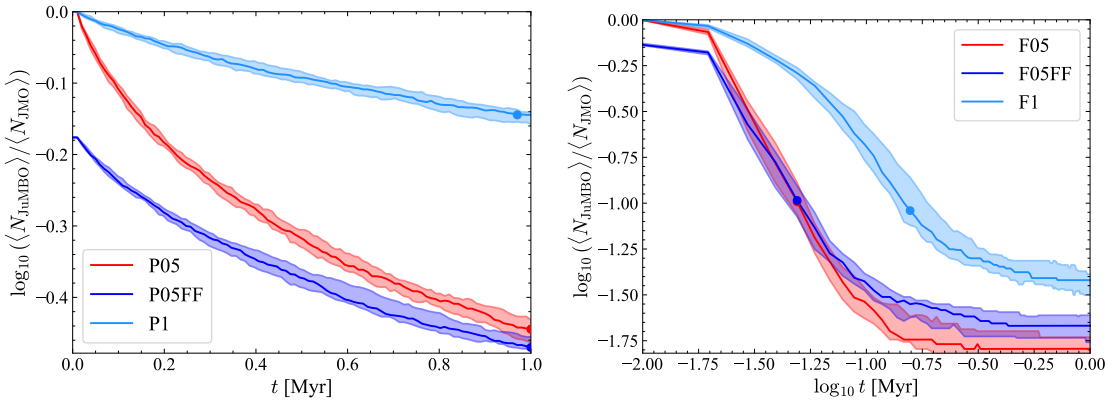

Figure 4: Fraction of jumbos as a function of time for models $\mathcal{ISF}$_Pl_R050 and $\mathcal{ISF}$_Pl_R100 (left panel, with a Plummer initial density profile), $\mathcal{ISF}$_Fr_R050 and $\mathcal{ISF}$_Fr_R100 (right panel) For model $\mathcal{ISF}$_Pl_R050 we also perform a calculation with a population of single Jupiter-mass objects. The number of free floating objects is the same as the number if primordial JuMBOs and their masses are taken from the primary mass function.

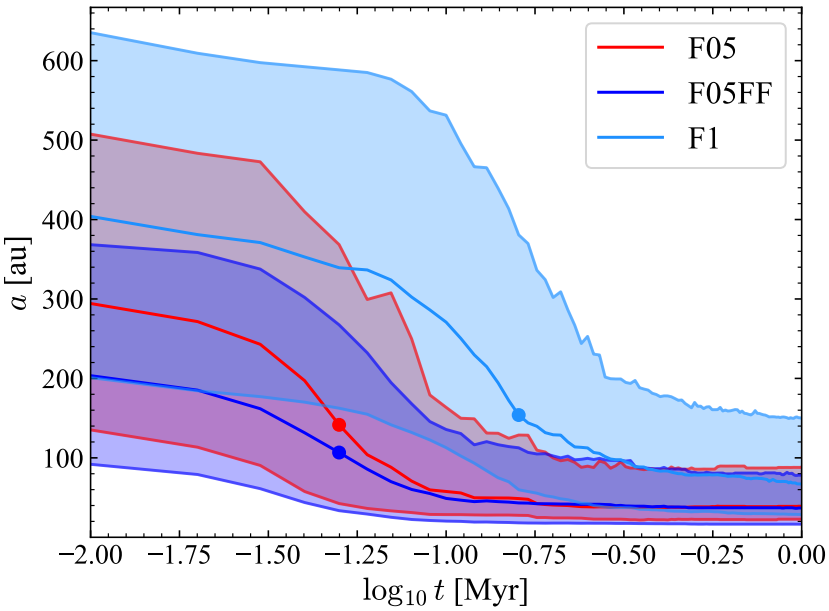

Figure 5: Evolution of the median orbital separation and the 20% and 75% quartiles of the distribution for model $\mathcal{ISF}$_Pl_R050 (red). In addition we show the model in which all JuMBOs were initially in circular orbits (light blue), and the model in which we constain the initial separation to 400 au rather than the generally adopted 1000 au.

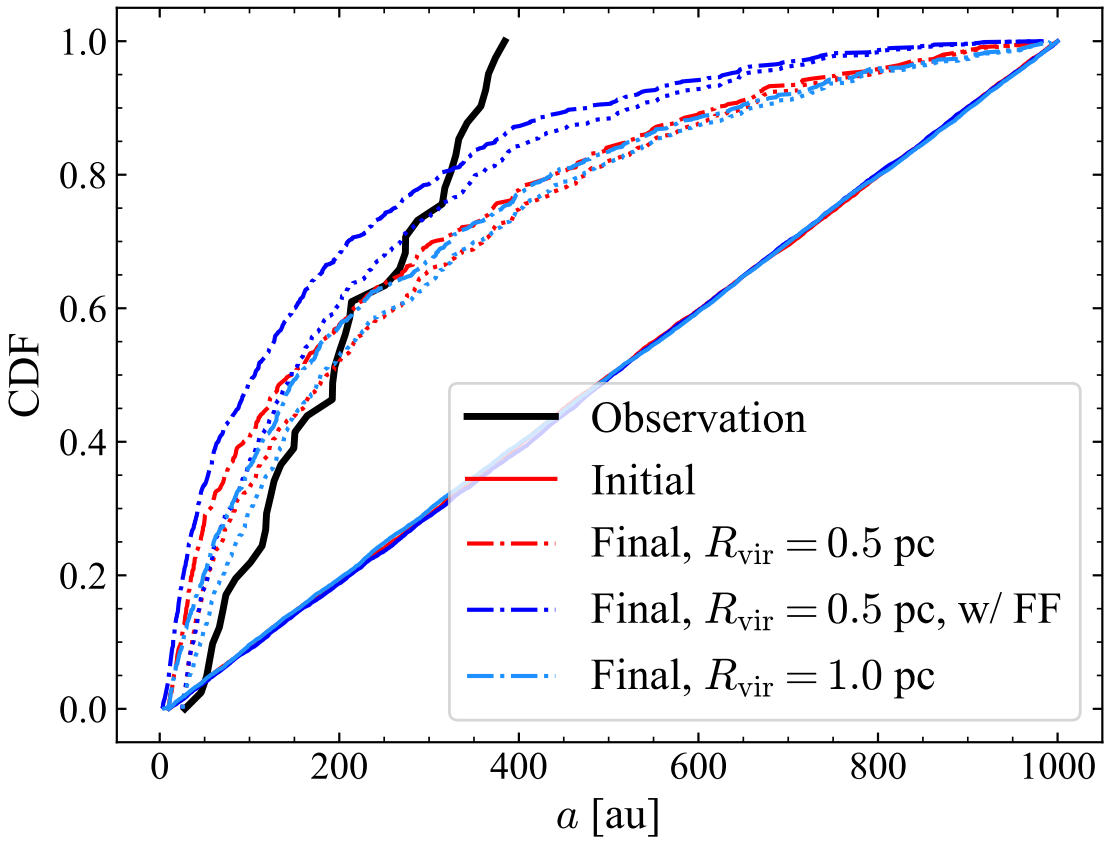

Figure 6: **ERWAN: Let's get rid of the dotted curves; reduces also the legend. Still need a caption. change CDF.**

the simulation, the widest orbits are being ionized, and by the time the cluster reaches an age of 1.0 Myr, the orbital distribution is skewed too much to lower values, compared to the observations. AT this age, however, the numbre of JuMBOs as well as their orbital separations matches the observed populations in the Trapezium cluster.

4.5 Introducing a population of free floaters in model $\mathcal{ISF}$

With the current models, we can further constrain the simulation parameters by repeating several calculations for better statistics and exploring other parts of the parameter space. We perform this analysis for model $\mathcal{ISF}$, because that model seems most promising for producing a sufficiently large population of JuMBOs in the range of observed parameters.

The orbital distribution of the surviving JuMBOs in the Plummer models is considerably more satisfactory than those that survive the fractal models (see figure 7). The tail to wider orbits, however, is more pronounced, potentially highlighting problems with initial conditions. Reducing the maximum orbital separation from 1000 au to 400 au helps resolving this discrepancy, but it seems a bit unfair to tune the initial conditions to mimick the observed parameters if the majority of primordial JuMBOs survives. It would be relatively straightforward to acquire a satifcatory comparison between simulations and observations if we start the simulations with a population of JuMBOs that reflects the observations.

Using the results of the models from section 4.1, we alter our initial conditions with the aim of mimicking observations. Doing so allows us to disentangle aspects of the cluster history, allowing for predictions on the properties of JuMBO formation.

Table 3: Statistics on the surviving JuMBOs. ⟨...⟩ gives the median, while the ± denote where the lower and upper quartiles. Col. 1: The fraction of JuMBOs present at the end of the simulation relative to the number initialised. Col. 2: The fraction of JuMBOs with projected separation, $r_{\rm ij} > 25$ au. Col. 3: The mass ratio of JuMBO systems. Col. 4: The primary mass of the JuMBO system. Col. 5: The semi-major axis of the JuMBO system. Col. 6: The eccentricity of the system. **ERWAN: should we get of the second column. Also, the caption needs work. I can do that.**

Model	$f_{\rm surv}$	$f_{r_{ij}\geq 25{\rm au}}$	$\langle M_{\rm prim}\rangle$ [$M_{\rm Jup}$]	$\langle M_{\rm sec}\rangle$ [$M_{\rm Jup}$]	r_{ij} [au]	$\langle a\rangle$ [au]	$\langle e\rangle$
Pl_050	$0.37^{+0.01}_{-0.02}$	$0.94^{+0.02}_{-0.01}$	$8.3^{+2.7}_{-3.1}$	$3.6^{+2.7}_{-1.8}$	233^{+234}_{-137}	268^{+237}_{-152}	$0.68^{+0.16}_{-0.22}$
Pl_050ff	$0.52^{+0.02}_{-0.00}$	$0.92^{+0.00}_{-0.01}$	$8.1^{+2.8}_{-3.2}$	$3.4^{+2.7}_{-1.7}$	162^{+167}_{-94}	187^{+176}_{-106}	$0.61^{+0.14}_{-0.18}$
Pl_100	$0.72^{+0.02}_{-0.01}$	$0.97^{+0.00}_{-0.01}$	$7.8^{+3.0}_{-3.0}$	$3.3^{+2.5}_{-1.6}$	344^{+271}_{-188}	396^{+250}_{-206}	$0.68^{+0.16}_{-0.20}$
Fr_050	$0.02^{+0.00}_{-0.00}$	$0.67^{+0.19}_{-0.07}$	$8.6^{+2.4}_{-3.3}$	$4.2^{+3.2}_{-1.9}$	38^{+52}_{-18}	39^{+50}_{-16}	$0.67^{+0.16}_{-0.19}$
Fr_050ff	$0.04^{+0.00}_{-0.01}$	$0.61^{+0.02}_{-0.11}$	$8.8^{+2.7}_{-2.6}$	$3.9^{+2.5}_{-2.0}$	30^{+43}_{-16}	37^{+41}_{-20}	$0.62^{+0.14}_{-0.21}$
Fr_100	$0.04^{+0.00}_{-0.01}$	$0.72^{+0.11}_{-0.06}$	$8.3^{+2.4}_{-3.0}$	$3.8^{+2.4}_{-1.9}$	64^{+98}_{-40}	67^{+83}_{-38}	$0.68^{+0.16}_{-0.19}$
Fr_050ffL	$0.03^{+0.00}_{-0.00}$	$0.46^{+0.07}_{-0.07}$	$8.1^{+2.9}_{-2.7}$	$2.7^{+3.1}_{-1.0}$	33^{+20}_{-18}	20^{+15}_{-9}	$0.61^{+0.20}_{-0.19}$
Pl_050ffO	$0.76^{+0.01}_{-0.01}$	$0.89^{+0.03}_{-0.03}$	$3.7^{+3.5}_{-2.1}$	$2.1^{+2.5}_{-1.2}$	90^{+86}_{-44}	105^{+86}_{-47}	$0.61^{+0.15}_{-0.17}$
Pl_050O	$0.02^{+0.00}_{-0.01}$	$1.00^{+0.00}_{-0.16}$	$4.0^{+2.6}_{-1.9}$	$2.8^{+1.7}_{-1.5}$	61^{+46}_{-24}	67^{+48}_{-22}	$0.67^{+0.14}_{-0.19}$
Fr_050ffO	$0.03^{+0.00}_{-0.00}$	$0.8^{+0.02}_{-0.15}$	$3.4^{+3.4}_{-1.7}$	$1.8^{+2.0}_{-0.8}$	44^{+37}_{-18}	46^{+38}_{-22}	$0.69^{+0.15}_{-0.18}$
Fl_050OC	$0.02^{+0.01}_{-0.00}$	$0.67^{+0.19}_{-0.07}$	$4.7^{+3.2}_{-2.7}$	$3.6^{+2.6}_{-2.02}$	46^{+36}_{-26}	49^{+28}_{-28}	$0.45^{+0.33}_{-0.23}$

We performed several simulatons with a virial radius of 0.5 pc and 1.0 pc and for Plummer as well as for fractal models. Some models were run with an additional population of single JMO's. In those cases, we often chose to have an equal number of JMO's as JuMBOs. The masses of these free floaters is identical to the JuMBO primaries, and they are distributed in the same density profile. These models, different from the $\mathcal{FFC}$ in that they still have a population of JuMBOs at the start. Each model calculation was repeated 10 times in order to build up a more reliable statistical sample.

For all models, we constrain $n_{\rm JuMBO} + n_{\rm FF}$ to values reflecting the total planetary-mass population observed in [1], keeping in mind the survival rate of JuMBOs based on previous results to decide on the initial value of $N_{\rm JuMBO}$. The range of primary and secondary masses is adapted to a flat distribution in masses in contrast to the power-law mass function in our earlier models (see section 3). The semi-major axis is uniformly distributed between the restricted range $a \in [25, 100]$ au, which is somewhat narrower than we adopted before in section 3. We run an additional series of simulations in which the primordial JuMBOs have an eccentricity beween 0.0 and 0.2 sampled from a uniform distribution, rather than the usual thermal eccentricity distribution. For the models that include free floating JMO's we add the designation "ff" to the model name, and the circular models recieve a letter 'c', for circular. The results of this series of $\mathcal{ISF}$ model calculations are summarized in table 3.

Adding a population of free floaters to the Plummer models, makes considerable difference in the evolution of the JuMBO fraction, but eventually, after about 1 Myr their fraction converges to roughly the same value. For models $\mathcal{ISF}$_Pl_R050 and $\mathcal{ISF}$_Fr_R050, illustrated in figure 4, this additional population of free floaters makes a considerable difference in the binary survival rate (see table 3).

It does make a difference in the orbital distribution of JuMBOs though, becasue the interaction between a relatively tightJuMBO with a relatively low-mass JMO could be hard, tightening

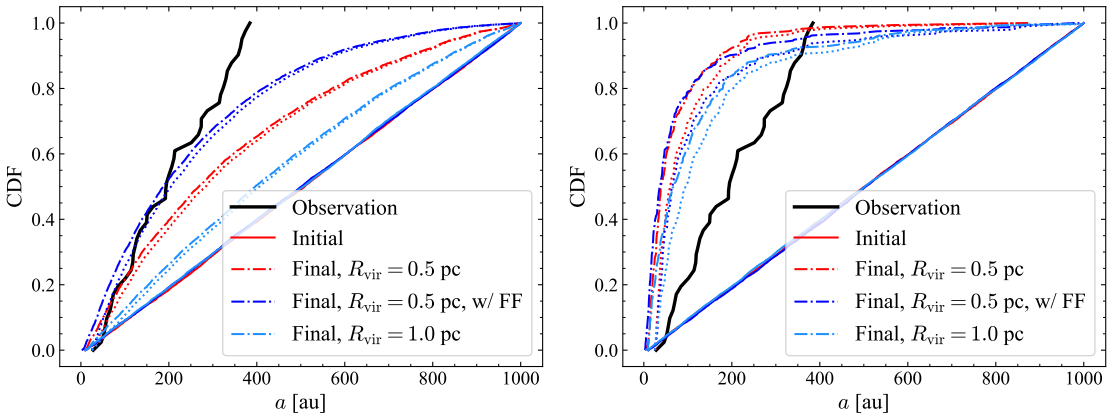

Figure 7: Cumulative distribution of surviving JuMBO semi-major axis distribution for models Pl_050, Pl_050ff, and Pl_100 (left panel), and Fr_050, Fr_050ff, Fr_100 (right panel). **ERWAN: replace the CDF axis labels.**

the JuMBO's orbit, whereas an encounter with a more massive object either widens the orbit or dissociates it.

More JuMBOs survive in the simulations that included a population of free floating JMOs. This increased surviveability may be the result of the hardening of the JuMBOs by occasional hard encounters with a JMO, making the former less vulnerable for ionization. The consequence of this hardening process is also visible in figure 7 where the JuMBOs in the models that included free floaters are on average tighter. This tightening of the orbits establishes itself already at a very early age, as can be seen in figure 6. The JuMBOs in these runs, however, remain soft for encounters with any of the stellar-mass objects in the cluster. The hardening then reduces the interaction cross section of the JuMBO making it less vulnerable for any interaction, including ionization.

The Fractal distribution efficiently prunes off any wide orbits since its violent nature provokes many encounters resulting in ionization. The tendency for JuMBOs to ionise at any encounter is reflected by the little variation between runs of the same virial radius. Also note the tendency for JuMBOs to ionise even when encountering a JMO. This is reflected in the models with free floating JMOs to have smaller orbital separations on average. This trend is even more clear in the Plummer models, see figure 7. where the orbital separations for models Pl_050 $\langle a \rangle \sim 296$ au compared to $\langle a \rangle \sim 187$ au for model Pl_050ff.

Including free floating JMOs then lead to more JuMBOs they have tighter orbits, and the widest orbits are ionized more effectively.

Increasing the number of JMOs also enhances the chances of two free-floaters settling into a newly formed binary, on average, only 0.40 new JuMBO systems emerge in models Fr_050 compared to the 0.65 in Fr_050ff. For the Plummer models the increased JuMBO formation rate is even more striking by increasing from 1.75 for model Pl_050 to 3.15 for model Pl_050ff. This result shaprly contrasts the $\mathcal{FFC}$ models, where, irrespective of how many JMOs we added to the cluster (up to 10^4) no JuMBOs formed in any of our simulations (see section 5.2 for a discussions). The primordial presence of JuMBOs mediates their further formation through interactions with JMOs.

In figure 8 we present the probability distrution of primary JuMBO mass and mass ratio for Plummer and fractal models. The observed point (red) seem to cover a similar parameter space, but overall distribution does not seem to be consistent with the observations. For the Plummer models this is, in principle, relatively simple to resolve, but using the observed distribution as input. For the fractal models such fine-tuning will be considerably harder because the fraction of

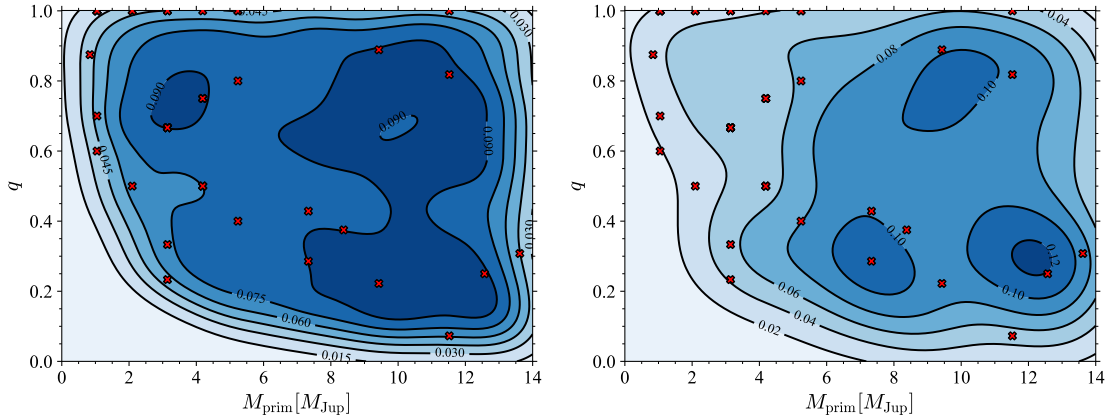

Figure 8: Probability distribution of primary mass versus mass ratio for the simulated JuMBOs in model $\mathcal{ISF}$_Pl_R050ff (blue contours). The red crosses show the observed JuMBOs. The primary masses for these runs ware generated from a uniform distribution, which is still evident in the Plummer model (left), but in the fractal model the initial conditions are lost.

survivers is only $\sim 4\,\%$.

The overabundance of equal-mass JuMBOs at $\lesssim 4\,M_{\rm Jup}$ primary masses in the observations is quite striking, and hard to explain. If not just statistics or observational bias, this could indicate some curious formation mechanism. The high-mass-ratio population JuMBOs is further illustrated in figure 9, where we plot the observed JuMBO population (data from [1]).

We could continue calibrating the initial conditions for a more consistent comparison with the observations, but the global parameter tuning seems to indicate that either the Plummer or the fractal models with a 0.5 pc virial radius compare most favorably to the observations. At this point, we do not see a natural mechanism to remove the tail of very wide-orbits among the JuMBOs, and it is a bit surprising that the observed orbital distribution seems to cut off rather sharply at about 400 au.

In figure 10 we show the primary mass function of the surviving JuMBOs for two models $\mathcal{ISF}$_Fr_R050. The initial distribution in presented as a solid curve, the final (after 1 Myr) as the dashed curve. The difference between initial and final mass primary function is not large; one tends to lose some objects in the low-mass end, causing the curve to become on average flatter, and the mean mass to increase. The two adopted initial primary mass funcitons were flat (red) and a power-law with an exponentn of -1.2. Although the global trends are similar, the steeper mass funcition leads to a better comparison with the observations. We do not present mass functions from the other simulations, because the trends are basically very similar.

5 Discussion

We explore the possible origin of the rich population of Jupiter-mass binary objects (JuMBOs) in the direction of the Trapezium cluster. The main problems in explaining the observations hides in the large number of Jupiter-mass objects, their large binary fraction and the wide separations. Assuming that they are bound, their orbits would be soft for any encounter in the cluster, and they are not expected to survive for more than a few hundred kyr (~ 0.4 Myr for Plummer models, and $\lesssim 0.1$ Myr for the 0.5 pc $\mathcal{ISF}$ fractal models).

The ease at which JuMBOs are ionized is illustrated in figure 4. It may be clear that the fractal models, due to their high frequency of strong encounters an the earliest cluster lifetime, have difficulty preserving wide planet-mass pairs. Plummer models are less dynamically interactive,

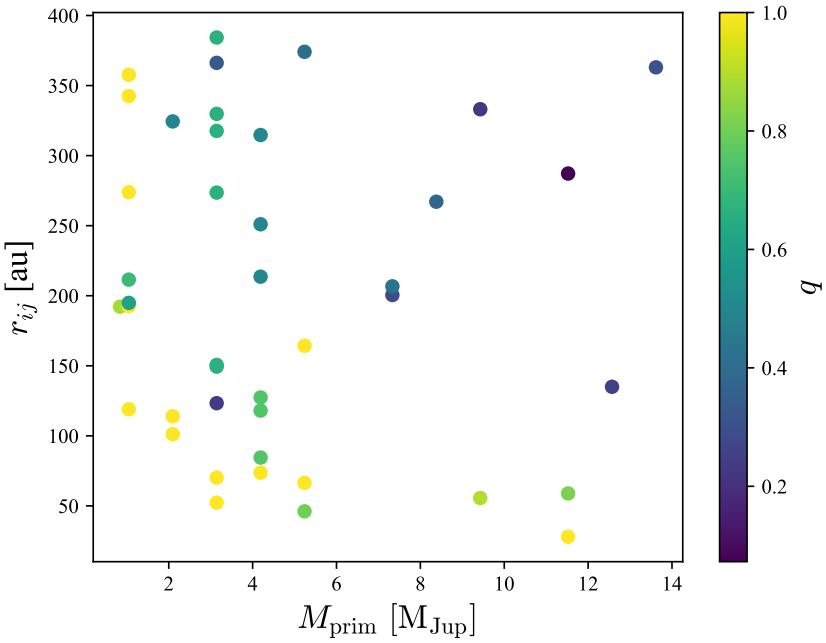

Figure 9: Distribution function of the observed JuMBOs, for primary mass, observed projected separation and mass-ratio (colors). The yellow bullet points indicate the high mass-ratio population, whereas the green/blue bullets show the low-mass ratio population. **ERWAN: Can you make the symbols larger?**

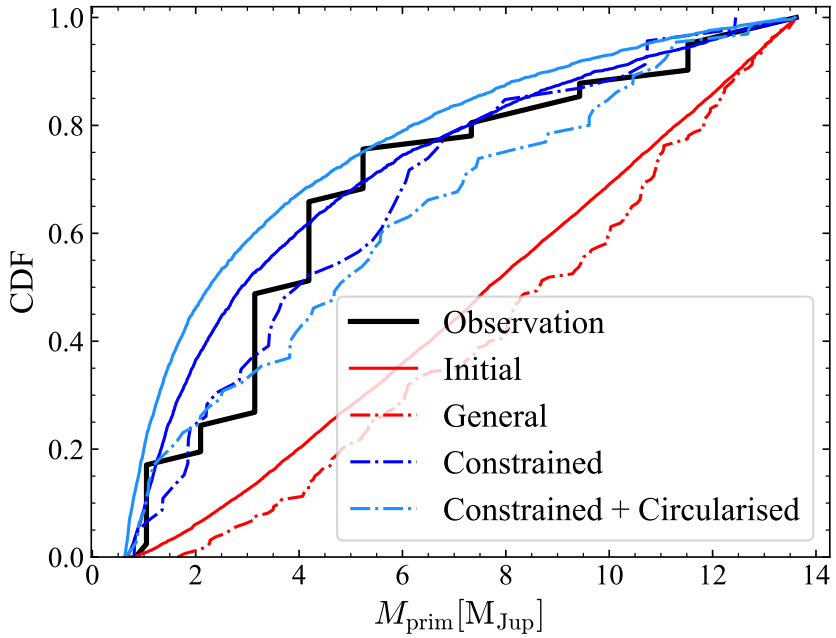

Figure 10: Distribution of the primary mass of the surviving JuMBO for models Fr_050 with an without an adapted mass function. The solid curves give the initial mass distribution, and the dashed curves the final (after 1 Myr). **ERWAN: Can we get rid of the light blue curve in the left panel?**

and the fraction of JuMBOs remains much higher, and even relatively wide pairs can survive.

An alternative explanation for the large population of pairs among the free-floating Jupiter-mass objects might be that they form late. If JuMBOs only formed in the last ~ 0.2 Myr They have a better chance to survive in the harsh cluster dynamical environment. Such a later formation would hardly affect the estimated mass of the objects, because the cooling curves, used to estimate their mass from the observed temperature and luminosity is rather flat at such young age [3].

The binary fraction continues to drop well after 0.2 Myr, and by the time the cluster is 1 Myr old only ~ 4 of the binraies in the fractal models survive. The survival fraction in the Plummer models is considerably higher, though. The fraction of JuMBO continues to drop, and by the time the cluster is ~ 11 Myr the fraction of jumbos is $\lesssim 2\,\%$. Interestingly enough, [5], reported the detection of 70 to 170 single Jupiter-mass objects in Upper Scorpius, which has an age of about 11 Myr. None of the objects in Upper Scorpius is paired, although this observation could be biased in terms of missing close pairs due to relatively low resolution of the observations. On the other hand, from the simulations, we would not expact many JuMBOs in Upper Scoprius. The binary fraction among the Jupiter-mass objects should be at most $\sim 2\%$. Upper Scoprius would then contain between 1 and 3 JuMBOs with an orbital separation $\gtrsim 25$ au. So far, none are observed.

On the other hand, our calculations, did not include primordial stellar binaries (or higher order systems), not did we take the effect of stellar evolution and supernovae into account. Those processes may have a profound effect of the fraction of JuMBOs, tending to reduce, rather then increase their number.

Starting with a large population of ($\gtrsim 600$) single free-floating planetary-mass objects among the stars (but without JuMBOs) would grossly underproduces the expected number of free floaters, and consquenty fails to reproduce the observed number of JuMBOs. This model, however, naturally leads to a mass-ratio distribution skewed to unity, as is observed. We consider this model undesireable by the lack of a large population of free-floating planets in the Trapezium cluster. This could indicate the existence of a large population of unobservable low-mass objects, but we consider this a rather exotic possibility.

5.1 Failure of model $\mathcal{SPP}$: star with a hierarchical planetary system

The $\mathcal{SPP}$ model systematically fail to reproduce the observed population of JuMBOs by a factor of 50 to 400. Changing the initial distribution in semi-major axis of the inner orbit from a uniform distribution to a logarithmic distribution reduces the formation rate of JuMBOs even further.

To further explore the failure of model $\mathcal{SPP}$, we perform an additional series of simulations in the Plummer distribution with virial radii of 0.25 pc, and 0.50 pc. According to [28], the eventual orbital separation of the JuMBO would be consistent with the difference in orbital separation between the two planets when orbiting the star. We performed dditional simulations with a mutual separation $a_2 - a_1 = 100$ au and $a_2 - a_1 = 200$ au, expecting those to lead to consistent results in comparison with the observed range in orbital separation for the JuMBOs, as was argued in [28]. The other orbital parameters, for the planet masses, their eccentricites and relative inclinations, in these models were identical to the other $\mathcal{SPP}$ models.

The results of these simulations are presented in figure 11. The JuMBO-formation efficiency for these models peaks for an orbital separation $a_1 \gtrsim 1000$ au, but steeply drops for smaller values of a_1. From a total of 45 calculations with various ranges of a_1 and a_2, 39 produced a total of 910 JuMBOs. The eventual distribution in separations is somewhat wider than claimed by [28], who argued that the initial orbital distance $a_2 - a_1$ would be preserved, but reasonably wise not inconsistent with the results of [28].

The rate, derived by [28], however, appears to be orders of magnitude smaller than they expected. They calculate the rate by means of 4-body scattering experiments, in which a star with two equal-mass planets with semi-major axes a_1 for the inner and a_2 for the other planet, encounters a single star. Their largest cross section of roughly a_1^2 is obtained if the encounter velocity

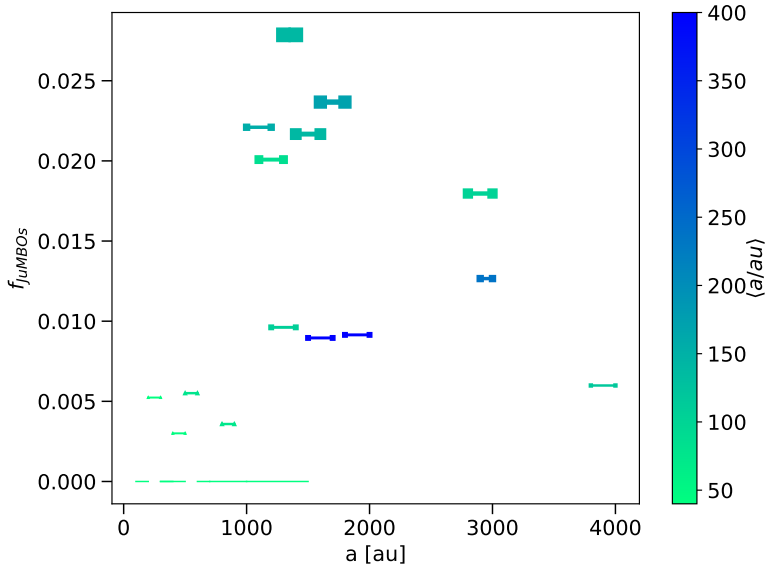

Figure 11: The number of jumbo's produced in model $\mathcal{SPP}$, as fraction of the number of free floating planets for various simulations starting with a Plummer sphere with a virial radius of 0.5 pc. The bullet points along each line correspond with the adopted orbital separation of the two planets (a_1 and a_2). The red symbols indicate an average orbital separations for the jumbos between 25 au and 380 au. The symbol sizes give the number of JuMBOs in these simulation linearly scales with a maximum of 9.

$0.8 v_\star / v_1$. For an encounter at the cluster's velocity dispersion, the inner planet would then have a orbital separation of ~ 900 au around a 1 $M_\odot$ star.

Note that an inner orbital separation of $a_1 = 900$ au for a 10 $M_{\rm Jup}$ planet leads to a Hill radius of about 160 au. An orbit with $a_2 = 1100$ au, is then rather unstable. Still, even in the runs where we use these parameters the total number of JuMBOs remains small compared to the number of free floaters. A stable hierarchical system of two Jupiter-mass planets in a circular orbit around a 1 $M_\odot$ star, would be dynamically stable if $a_1 \simeq 120$ au and $a_2 \simeq 210$ au. Even if each star in the Trapezium cluster was born with two such planets at most one third of the 42 observed JuMBOs could conceivably be explained, and the number of free floating JMOs would run in the thousands.

The results of the cross section calculations performed by [28] are consistent with our direct N-body simulation, but that the adopted initial orbital separation is too wide in comparison with a realistic population of inner planetary orbits for Jupiter-mass objects. Observational selection effect in finding $\gtrsim 900$ au JMOs are quite severe, but we consider it unrealistic to have 300 out of 2500 stars to be orbited by such wide planetary systems. In particular, when one considers the small sizes of the observed disks in the Trapezium cluster, which today are all smaller than 400 au [47].

5.2 Failure of model $\mathcal{FFC}$: Free-Floating Jupiter-Mass Objects

In scenario, $\mathcal{FFC}$, we initialize 600 to 10^4 single Jupiter-mass objects in a cluster of stars without JuMBOs (see section 3.1), expectating that some soft pairs form naturally through interactions with the stars. Soft binary formation, through three-body interactions is not expected to be very effective [48], but with a sufficiently large population, one might expect a few JuMBOs to form. Potentially, some of the observed JuMBOs originate from this process.

A JuMBO can form in models $\mathcal{FFC}$, when two JMO and a single star happen to occupy the

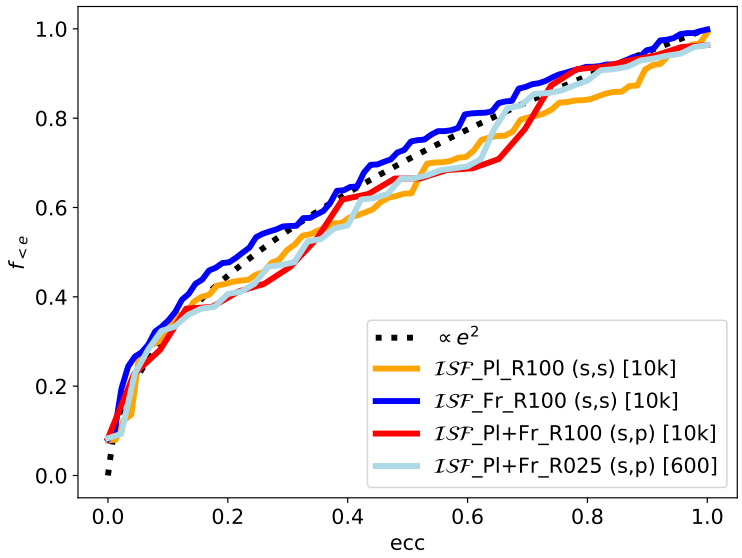

Figure 12: Eccentricity distribution for several models (indicated in the lower right inset) for stellar binaries and captured planet-mass objects. Overplotted, for comparison, is the thermal distribution.

same phase space volume, in which case the star can escape with the excess angular momentum and energy, leaving the two planet-mass objects bound. The distance at which a JMO with mass m and a star with mass M can be considered bound can be estimated from the 90° turn-around distance, which is $r_{90} = G(M + m)/v^2$. For our adopted clusters $r_{90} \simeq 900$ au. Following [48], we estimate the probability of this to happening at $\sim 10^{-2}$ per JMO per relaxation time. The relaxation time of our Trapezium model cluster is approximately $t_{\rm rlx} \propto N/(6\ln(N))t_{\rm cross} \sim 64 t_{\rm cross}$. With a crossing time of about 1 Myr (roughly the crossing time for our 1 pc models) we expect ~ 0.5 JuMBOs to form. The estimates by [48] adopted equal mass objects, but the more detailed numerical study, carried out by [49], arrive at a similar number of soft binaries. The latter study, however, focused on post core collapsed clusters, which is not appropriate for our Plummer models, but more in line with our fractal models. Stellar sub-clumps collapse in the fractal models within ~ 0.2 Myr, mimicking the post collapse evolution as addressed in [49]. In principle, their model, therefore, is somewhat appropriate to our $\mathcal{FCC}$ models.

Interestingly enough, the $\mathcal{FFC}$ models produce quite a rich population of stellar pairs (82.8 ± 6.6) and several cases where a JMO is captured by a star (6.5 ± 3.3) for the Plummer as well as for the fractal models. But no JuMBOs formed. In higher abundance of stellar pairs compared to planetary captures is somewhat unexpected. In figure 12 we present the cumulative distribution of the eccentricities found in several of our model calculations. Each of them is consistent with the thermal distribution (indicated as the black dotted curve).

The secondary masses in the stellar pairs that formed are statistically indistinguishable from the primary masses of the stars that captured a planet, and their orbits a wider; 182 ± 67 au for the binaries and 288 ± 164 au for the captured JMOs. With the higher masses the binaries are roughly 100 times harder than the JMO captured systems; straddling the hard-soft boundary.

5.3 The long-term surviveability if JuMBOs

To study the long-term survivability of JuMBOs we continue 5 runs for each of the models $\mathcal{ISF}$_Pl_050 and $\mathcal{ISF}$_Fr_050 until an age of 10 Myr. Our aim is to look at the survival of

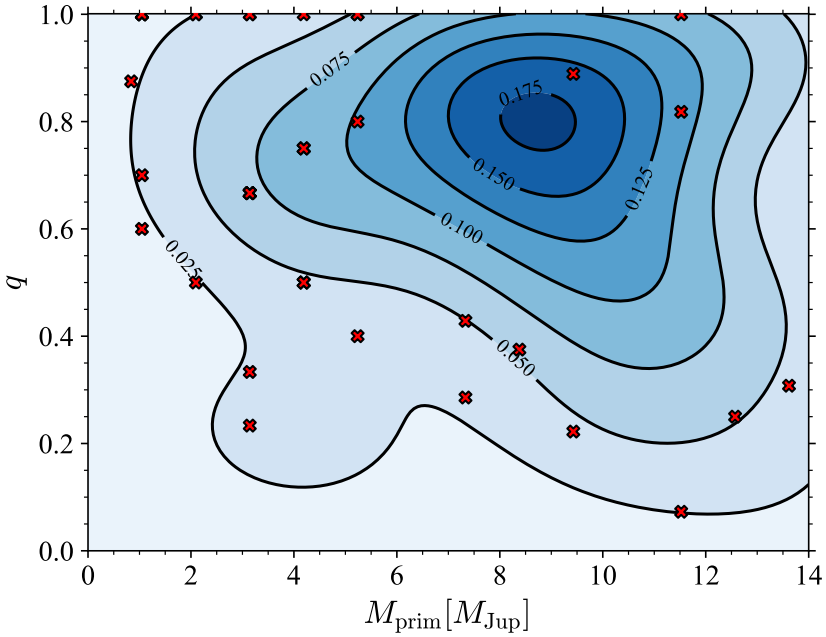

Figure 13: Distribution of primary mass versus the mass ratio for model $\mathcal{ISF}$_Fr_050ff at an age of 10 Myr. Note that here we adopted the power law ($\alpha = -1.2$) mass function for the primaries. Red crosses denote where observed JuMBOs lie.

JuMBOs in older systems systems, such as Upper Scoprius. Overall, the JuMBO survival rate decreases rapidly, with a half-life time < 1 Myr, and the survivers have tighter orbits. The population of JuMBOs eventually settles at a population of dynamically hard pairs, in which case the mean orbital separation $\langle a \rangle \lesssim 20$ au for two 3 $M_{\rm Jup}$ objects. The hardness of these pairs is mostly the result of the decrease in the cluster density with time, rather than in the shrinking of the surviving JuMBOs.

In figure 13 we present the distribution in primary mass and mass ratio for simulation $\mathcal{ISF}$_F050ff at an age of 10 Myr (adopting the power-law primary mass function). The younger equivalent, at an age of 1 Myr and adopting a flat mass function for the primaries is presented in the left panel of figure 8. The most likely survivors have high primary and secondary masses, as could be expected based on the hardness of these systems, which is seen in figure 13.

5.4 Observational Constraints

ERWAN: This paragraph still needs work, and maybe it would be merged with the next paragraph

When fine-tuning the initial conditions, $f_{\rm surv}$ and e barely changes while a shows only marginal changes. This slight increase in $f_{r_{ij}\geq 25\text{ au}}$, $\langle a \rangle$ and $\langle r_{ij} \rangle$ could be attributed to the reduction of JMO and JuMBOs present in the environment and the smaller masses they occupy making it harder for them to ionize binaries. The difference in the semi-major axis distribution between models Fr_050 with JuMBOs initially on eccentric or circular orbits, is shown in figure 14. The Fractal models exhibit a natural tendency for trimming out wide binaries.

No matter the initial configuration of JuMBOs, a similar evolution is observed where surviving JuMBOs tend to have larger primary masses. However, unlike the F05 model, the constrained model, initialised with $\alpha = -1.25$, end up being roughly uniform in primary mass compared to the somewhat thermal appearance for F05. In doing, the median primary masses shift towards lower values while the mass ratio towards larger one. A fact reflected by the statistics shown in table 3

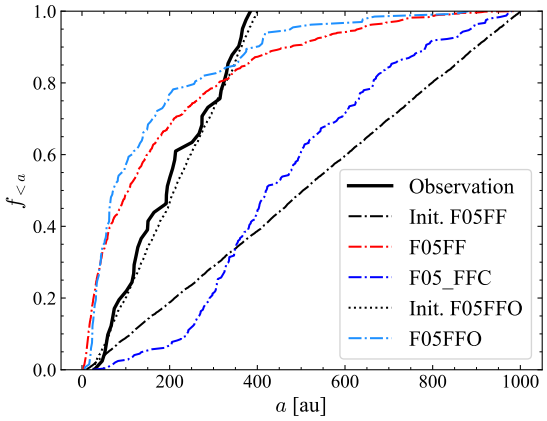

Figure 14: Cumulative distributions for the orbital separation for the models Fr_050ff. **ERWAN: I am not 100% sure what this plot shows. Is it the distro from fractals at 0.2Myr?**

Table 4: TO CHECK **ERWAN: I thikn that this table can go** .

Model	$\langle N_{\rm JS,merge}\rangle$	$\langle N_{\rm SS,merge}\rangle$	$\langle N_{\rm JS}\rangle$	$\langle N_{\rm multi}\rangle$
F05	$2.5^{+0.5}_{-1.5}$	19^{+4}_{-7}	8^{+3}_{-0}	2^{+0}_{-0}
F05FF	$5.5^{+1.5}_{-1.5}$	21^{+2}_{-4}	14^{+1}_{-3}	2^{+0}_{-0}
F1	$1.0^{+1.0}_{-0.0}$	14^{+3}_{-5}	10^{+1}_{-3}	2^{+0}_{-0}
F05FFL	$5.0^{+0.0}_{-1.0}$	22^{+3}_{-5}	$1.0^{+0.0}_{-0.0}$	0^{+7}_{-0}
F05O	$2.0^{+0.8}_{-1.8}$	25^{+2}_{-8}	$4.5^{+2.8}_{-0.5}$	2.0^{+0}_{-0}
F05FFO	$1.0^{+1.0}_{-0.0}$	17^{+3}_{-1}	$5.0^{+1.5}_{-1.0}$	1.0^{+0}_{-0}
F05OC	$0.5^{+2.3}_{-0.5}$	20^{+5}_{-4}	$4.5^{+1.5}_{-1.5}$	3.5^{+0}_{-0}

and shown in figure 15.

Although, in this model, we aimed at reproducing the primary mass-function and mass ratio distribution, we clearly under represent high mass primaries witha low mass ratio. For the Plummer models it will be relatively streightforward to reproduce both populations (the high mass ratio, as well as those with a low mass ratio), but in the fractal models the survival rate is too low to still reflect the initial conditions.

The statistics of merging scenarios, and the emergence of both Jupier-mass - Stellar binary systems and $N \geq 3$ systems are summarised in table 4.

In figure 16, we present the distribution of the surviving JuMBOs in semi-major axis and eccentricity. The stellar binaries occupy roughly the same space. The parameter space is widely covered, with signs of low-eccentricity but very wide ($a \geq 700$ au) binaries. Nevertheless, the vast majority exhibit large eccentricities and semi-major axis, reflecting their dynamical origin. The non-negligible amount of these systems emerging provide an interesting prospect of detecting ultra-cold Jupiters orbiting stars who have recently fostered them.

Given the poor reproducability in ratios of JuMBOs to JMO free floaters and the tight orbits of JuMBOs we conclude that the $\mathcal{ISF}$ models are most likely not the origins of JuMBOs, lending us to our final possible scenario, $\mathcal{FFC}$.

Our slight preference for the fractal models stems from their natural consequence of producing higher order hierarchical systems. Much in the same was as the two triple JuMBOs (Jupiter-mass

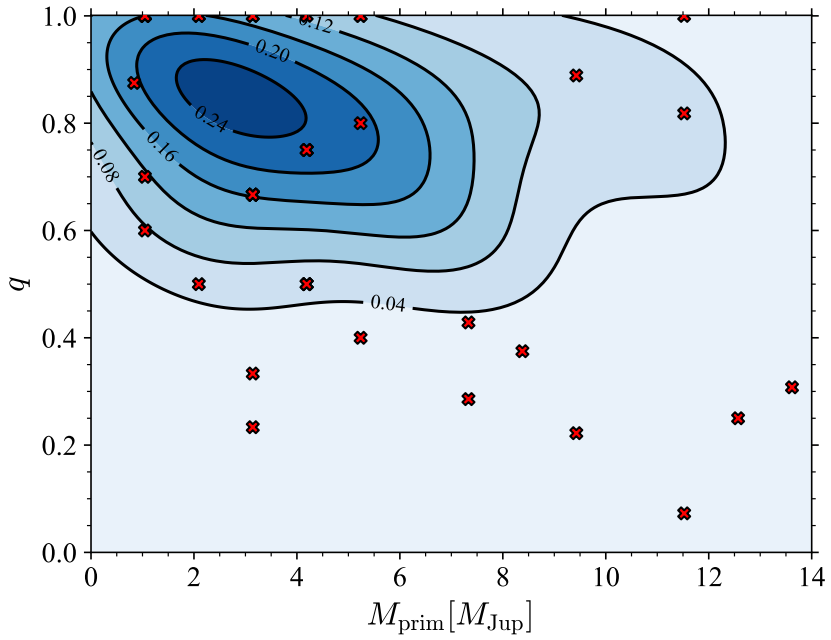

Figure 15: Contours of constant density in the plane of primary mass versus mass-ratio for model $\mathcal{IMF}_050$ff. Red crosses denote where observed JuMBOs. In this model, the initial mass function and mass-ratio distributions for the JuMBOs were skewed to lower mass primararies ($\alpha = -1.2$), and to equal mass systems (q between 0.2 and 1.0 from the thermal distribution.

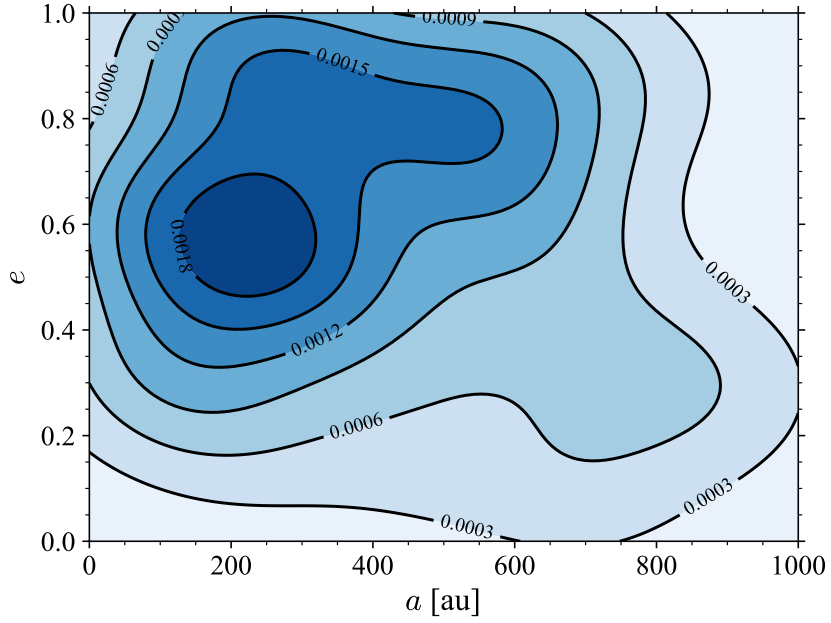

Figure 16: Contours of constant density for semi-major axis and eccentricities for stars that managed to capture a JMO for model $\mathcal{IMF}_050$ff. These systems are suprisingly common in our simulations, and they even tend to be rather tight. The actual orbits are still dynamicall soft, though..

Triple Objects, JuMTO). In none of the Plummer models formed any triples, however, a seizable fraction of primordial triples may survive: we are then back at weighting the relative importance of initial conditions versus dynamical evolution.

5.5 Assessment on the origin of JuMBOs

In the $\mathcal{ISF}$ Plummer models, $\sim$ 61% of the JuMBOs are ionized within 1 Myr, compared to $\sim$ 96 % for the fractal models. The observed population of free floaters and JuMBOs can then be reproduced if the cluster was born with half the free floating as Jupiter-mass planets and half as pairs. The current observed primary and secondary masses of JuMBOs would then still reflect the conditions at birth, but the semi-major axis and eccentricity distributions would have been affected considerably by encounters with other cluster members. These processes tend to drive the eccentricity distribution to resemble the thermal distribution (probably with an excess of $\gtrsim 0.7$ eccentricities [50]). The semi-major axes of the jumbos would have widened, on average by approximately 5% due to encounters with free-floating planet-mass objects.

Alternative to a Plummer initial stellar distribution we consider fractal distributions, which are also able to satisfactorily reproduce the observed populations. In the fractal models, $\sim$ 90 % of the priordial JuMBOs become ionized, and in principle the entire observed populations of free-floating Jupiter mass objects and JuMBOs can be explained by a 100% initial binarity among the JuMBOs. We then conclude that single Jupiter mass objects are preferentially born in pars with a rather flat distribution in orbital separations with a maximum of $\sim$ 400 au. Higher order multiplicity (triple JuMBOs) form naturally from interactions between two or more JuMBOs in the fractal models.

This model satisfactorily explains the observed orbital separation distribution, with a $\sim$ 15% excess of systems with a separation $\gtrsim$ 400 au. We do not expect a rich population of orbits with separation smaller than the observed 25 au. The fraction of pairs among the wide systems is already high, and there are simply not enough single JMOs observed to accomodate this tight binary population, except if a considerable fraction of the single observed JMOs are in fact such tight binaries.

We have a slight preference for the $\mathcal{ISF}$ fractal models with 0.5 pc virial radius because hierarchical triple JMOs form naturally in roughly the observed proportion (on average $\sim$ 4 triples among $\sim$ 40 pairs and $\sim$ 500 single JMOs). The singles then originate from broken-up pairs, and the trples form in interactions between two JMO pairs. The dynamical formation of soft triple JMOs is quite remarkable, and observational follow-up would be of considerable interest.

The mass function of the single JMOs then should resemble the combined mass functions of the primary and secondary masses of the JuMBOs. The ionization probability for a JuMBO does not depend on its mass, but on the chance coincidence of meeting a star, and the majority of JMOs seem to have come from ionized JuMBOs.

The short-periods and the small binary fraction of the fractal models could be salvaged if the JuMBOs form late. If the majority of the observed population formed $\lesssim$ 0.2 Myr ago, the cluster's density profile would already have been smoothed out, leading to fewer strong dynamical encounters. The cluster would somewhat resemble a JuMBO-friendly Plummer-like structure. Not only would that mediate the survival of JuMBOs but it also would allow them to preserve their wide orbits, as observed.

6 Conclusions

The discovery of 40 relatively wide pairs and 2 triples of Jupiter-mass objects in the Trapezium cluster emphasizes our limited understanding of low-mass star and high-mass planet formation. In order to derive characteristcs for their origin we performed simulations of Trapezium-equivalent

stellar clusters (2500 stars in a virialized 0.25 pc to 1.0 pc radius) with various compositions of Jupiter-mass objects and stars.

Models in which planets form in wide hierarchical circum-stellar orbits (model $\mathcal{SPP}$), as proposed by [28], produce many single free floating planets, but insufficient numbers of pairs. The ratio of single to pairs of planet-mass objects in these models is too low by a factor of 50 to 400, irrespective of the initial stellar distribution function.

The models in which pairs of planetary-mass objects orbit stars in the form of a planet-moon system (or binary planets, model $\mathcal{SPM}$), produce a sufficent number of free-floating planetary pairs, and cover the proper range of orbits. In particular the models that start with fractal initial conditions tend to produce a sufficent fraction of JuMBOs among free-floating objects $O(0.1)$, which is close to the observed value of 0.078 ± 0.012. In the Plummer distribution, the number of stars that survive with at least one planet-mass objects is considerable. In general, these models predict low-eccentricities ($e \lesssim 0.4$), whereas others lead to thermalized distributions ($e \gtrsim 0.6$).

For model $\mathcal{SPM}$ to produce a sufficient number of JuMBOs it requires planet-moon pairs to form in $\gtrsim 900$ au orbits around their parent star. Such wide orbits are exotic considering the fact that the circum-stellar disks observed in the Trapezium cluster tend to be smaller than 400 au. We therefore do not see how such wide planet-moon pairs can form around stars. If, however, such binary-planets, are found in the Trapezium cluster we do consider this model a serious candidate for producing JuMBOs. Investigating some of the observed JuMBOs in the images published in [1], we do get the impression that some JuMBOs may have nearby stars, but a thorough statistical study to confirm this correlation is necessary. Model $\mathcal{SPM}$ can easily be confirmed or ruled out by establishing the existence of those left over (or dynamically formed) planetary systems.

Ruling out models $\mathcal{FFC}$, $\mathcal{SPP}$, and possibly $\mathcal{SPM}$, we are left with the simplest solution; JuMBOs form together with the single stars in the cluster. This model reproduces the observed rates and orbital characteristics (a bit by construction, though), it can also be used to further constrain the initial conditions of the cluster as well as the JuMBOs.

Single free floating planetary objects were discovered in abundance (between 70 and 170 candidates) before in the Upper Scorpius association [5], but these were considered to be single free floaters. With an age of about 11 Myr [5], Upper Scoprius is expected to be rich in single Jupiter-mass free floating planets, but binaries will be rare as the majority will be ionized. We still could imagine that a few JuMBOs have survived until today.

Finally, we would like to comment briefly on the nature of the objects observed. We wonder that, if these objects formed in situe, and therefore not around a star, they would be deprived of a rocky core. JuMBOs and JMOs would then more resemble a star in terms of the structure, rather than a planet. This may have interesting consequences on their dynamics, their evolution, and when they encounter another star (collisions in our simulations are relatively frequent). In those terms, we also wonder to what degree the term "planet" is rectified at all, and maybe it is time to revive the IAU discussion on the definition of a planet.

We tend to prefer model $\mathcal{ISF}$ with a 0.5 pc Plummer sphere because it can be tuned rather easily to reproduce the observed population of JuMBOs and JMOs. On the other hand, we also consider the equivalent fractal model a good candidate. We had greater difficulty reproducing the observed JuMBOs but they naturally lead to some Jupiter-Mass Triple Objects (JuMTOs). To make the fractal model work, we can prefer JuMBOs to form relatively late compared to the other stars in the cluster.

Software used for this study

In this work we used the following packages: `python` [51], `AMUSE` [44], `numpy` [52], `scipy` [53], `matplotlib` [54].

Energy Consumption

`ERWAN: We'll have to rewrite this.`

The 820 simulations conducted during this investigation had a total wall-clock time of 432 days. For the XYZ runs, each CPU used 6 cores, for the other two configurations 18 cores were used per CPU. In total, the CPU time for all simulations was 7680 days. Assuming a CPU consumption rate of 12 Watt hr^{-1} [55], the total energy consumption is roughly 2210 kWh. For an emission intensity of 0.283 kWh kg^{-1} [56], our calculations emitted 7.8 tonnes of CO2, roughly equivalent to two round trips by plane New York - Beijing.

Acknowledgments

We are grateful to Veronica Saz Ulibarrena, Shuo Huang, Maite Wilhelm, Brent Maas, and Samuel Pearson for being available to discussing JuMBOs with us. We thank NOVA for support.

References

[1] S. G. Pearson and M. J. McCaughrean, *Jupiter Mass Binary Objects in the Trapezium Cluster*, arXiv e-prints arXiv:2310.01231 (2023), doi:10.48550/arXiv.2310.01231, `2310.01231`.

[2] M. R. Zapatero Osorio, V. J. S. Béjar, E. L. Martín, R. Rebolo, D. Barrado y Navascués, C. A. L. Bailer-Jones and R. Mundt, *Discovery of Young, Isolated Planetary Mass Objects in the σ Orionis Star Cluster*, Science **290**(5489), 103 (2000), doi:10.1126/science.290.5489.103.

[3] P. W. Lucas and P. F. Roche, *A population of very young brown dwarfs and free-floating planets in Orion*, MNRAS **314**, 858 (2000), doi:10.1046/j.1365-8711.2000.03515.x, `arXiv:astro-ph/0003061`.

[4] R. Mundt, C. A. L. Bailer-Jones, M. R. Zapatero Osorio, V. J. S. Béjar, R. Rebolo, D. Barrado Y Navascués and E. L. Martin, *Discovery of Very Young Free-floating Giant Planets in the σ Orionis Cluster*, In *Astronomische Gesellschaft Meeting Abstracts*, vol. 17 of *Astronomische Gesellschaft Meeting Abstracts* (2000).

[5] N. Miret-Roig, H. Bouy, S. N. Raymond, M. Tamura, E. Bertin, D. Barrado, J. Olivares, P. A. B. Galli, J.-C. Cuillandre, L. M. Sarro, A. Berihuete and N. Huélamo, *A rich population of free-floating planets in the Upper Scorpius young stellar association*, Nature Astronomy **6**, 89 (2022), doi:10.1038/s41550-021-01513-x, `2112.11999`.

[6] T. Sumi, K. Kamiya, D. P. Bennett, I. A. Bond, F. Abe, C. S. Botzler, A. Fukui, K. Furusawa, J. B. Hearnshaw, Y. Itow, P. M. Kilmartin, A. Korpela *et al.*, *Unbound or distant planetary mass population detected by gravitational microlensing*, Nat **473**, 349 (2011), doi:10.1038/nature10092, `1105.3544`.

[7] N. Miret-Roig, *The origin of free-floating planets*, Ap&SS **368**(3), 17 (2023), doi:10.1007/s10509-023-04175-5, 2303.05522.

[8] C. Low and D. Lynden-Bell, *The minimum Jeans mass or when fragmentation must stop.*, MNRAS **176**, 367 (1976), doi:10.1093/mnras/176.2.367.

[9] D. F. A. Boyd and A. P. Whitworth, *The minimum mass for opacity-limited fragmentation in turbulent cloud cores*, A&A **430**, 1059 (2005), doi:10.1051/0004-6361:20041703, astro-ph/0411495.

[10] C. Chen, R. G. Martin, S. H. Lubow and C. J. Nixon, *Tilted circumbinary planetary systems as efficient progenitors of free-floating planets*, arXiv e-prints arXiv:2310.15603 (2023), 2310.15603.

[11] A. van Elteren, S. Portegies Zwart, I. Pelupessy, M. X. Cai and S. L. W. McMillan, *Survivability of planetary systems in young and dense star clusters*, A&A **624**, A120 (2019), doi:10.1051/0004-6361/201834641, 1902.04652.

[12] F. A. Rasio and E. B. Ford, *Dynamical instabilities and the formation of extrasolar planetary systems*, Science **274**, 954 (1996), doi:10.1126/science.274.5289.954.

[13] X. Zheng, M. B. N. Kouwenhoven and L. Wang, *The dynamical fate of planetary systems in young star clusters*, MNRAS **453**, 2759 (2015), doi:10.1093/mnras/stv1832, 1508.01593.

[14] J. R. Hurley and M. M. Shara, *Free-floating Planets in Stellar Clusters: Not So Surprising*, ApJ **565**, 1251 (2002), doi:10.1086/337921, astro-ph/0108350.

[15] M. X. Cai, M. B. N. Kouwenhoven, S. F. Portegies Zwart and R. Spurzem, *Stability of multi-planetary systems in star clusters*, MNRAS **470**, 4337 (2017), doi:10.1093/mnras/stx1464, 1706.03789.

[16] F. Flammini Dotti, M. B. N. Kouwenhoven, M. X. Cai and R. Spurzem, *Planetary systems in a star cluster I: the Solar system scenario*, MNRAS **489**(2), 2280 (2019), doi:10.1093/mnras/stz2346, 1908.07747.

[17] A. P. Whitworth and D. Stamatellos, *The minimum mass for star formation, and the origin of binary brown dwarfs*, A&A **458**(3), 817 (2006), doi:10.1051/0004-6361:20065806, astro-ph/0610039.

[18] E. B. Ford, M. Havlickova and F. A. Rasio, *Dynamical Instabilities in Extrasolar Planetary Systems Containing Two Giant Planets*, Icarus **150**(2), 303 (2001), doi:10.1006/icar.2001.6588, astro-ph/0010178.

[19] W. Hao, M. B. N. Kouwenhoven and R. Spurzem, *The dynamical evolution of multiplanet systems in open clusters*, MNRAS **433**, 867 (2013), doi:10.1093/mnras/stt771, 1305.1413.

[20] K. Stock, M. X. Cai, R. Spurzem, M. B. N. Kouwenhoven and S. Portegies Zwart, *On the survival of resonant and non-resonant planetary systems in star clusters*, MNRAS **497**(2), 1807 (2020), doi:10.1093/mnras/staa2047, 2007.11601.

[21] J. D. Kirkpatrick, C. R. Gelino, J. K. Faherty, A. M. Meisner, D. Caselden, A. C. Schneider, F. Marocco, A. J. Cayago, R. L. Smart, P. R. Eisenhardt, M. J. Kuchner, E. L. Wright *et al.*, *The Field Substellar Mass Function Based on the Full-sky 20 pc Census of 525 L, T, and Y Dwarfs*, ApJS **253**(1), 7 (2021), doi:10.3847/1538-4365/abd107, 2011.11616.

[22] W. M. J. Best, M. C. Liu, T. J. Dupuy and E. A. Magnier, *The Young L Dwarf 2MASS J11193254-1137466 Is a Planetary-mass Binary*, ApJL **843**(1), L4 (2017), doi:10.3847/2041-8213/aa76df, 1706.01883.

[23] C. Beichman, C. R. Gelino, J. D. Kirkpatrick, T. S. Barman, K. A. Marsh, M. C. Cushing and E. L. Wright, *The Coldest Brown Dwarf (or Free-floating Planet)?: The Y Dwarf WISE 1828+2650*, ApJ **764**(1), 101 (2013), doi:10.1088/0004-637X/764/1/101, 1301.1669.

[24] P. Calissendorff, M. De Furio, M. Meyer, L. Albert, C. Aganze, M. Ali-Dib, D. C. Bardalez Gagliuffi, F. Baron, C. A. Beichman, A. J. Burgasser, M. C. Cushing, J. K. Faherty *et al.*, *JWST/NIRCam Discovery of the First Y+Y Brown Dwarf Binary: WISE J033605.05-014350.4*, ApJL **947**(2), L30 (2023), doi:10.3847/2041-8213/acc86d, 2303.16923.

[25] K. Kellogg, S. Metchev, P. A. Miles-Páez and M. E. Tannock, *A Statistical Survey of Peculiar L and T Dwarfs in SDSS, 2MASS, and WISE*, AJ **154**(3), 112 (2017), doi:10.3847/1538-3881/aa83b0, 1708.03688.

[26] S. C. Eriksson, M. Janson and P. Calissendorff, *Detection of new strongly variable brown dwarfs in the L/T transition*, A&A **629**, A145 (2019), doi:10.1051/0004-6361/201935671, 1910.02638.

[27] C. Clanton and B. S. Gaudi, *Synthesizing Exoplanet Demographics: A Single Population of Long-period Planetary Companions to M Dwarfs Consistent with Microlensing, Radial Velocity, and Direct Imaging Surveys*, ApJ **819**(2), 125 (2016), doi:10.3847/0004-637X/819/2/125, 1508.04434.

[28] Y. Wang, R. Perna and Z. Zhu, *Floating binary planets from ejections during close stellar encounters*, arXiv e-prints arXiv:2310.06016 (2023), doi:10.48550/arXiv.2310.06016, 2310.06016.

[29] M. B. N. Kouwenhoven, S. P. Goodwin, R. J. Parker, M. B. Davies, D. Malmberg and P. Kroupa, *The formation of very wide binaries during the star cluster dissolution phase*, MNRAS **404**(4), 1835 (2010), doi:10.1111/j.1365-2966.2010.16399.x, 1001.3969.

[30] H. B. Perets and M. B. N. Kouwenhoven, *On the Origin of Planets at Very Wide Orbits from the Recapture of Free Floating Planets*, ApJ **750**, 83 (2012), doi:10.1088/0004-637X/750/1/83, 1202.2362.

[31] N. Goulinski and E. N. Ribak, *Capture of free-floating planets by planetary systems*, MNRAS **473**(2), 1589 (2018), doi:10.1093/mnras/stx2506, 1705.10332.

[32] S. F. Portegies Zwart, *Stellar disc destruction by dynamical interactions in the Orion Trapezium star cluster*, MNRAS **457**, 313 (2016), doi:10.1093/mnras/stv2831, 1511.08900.

[33] H. C. Plummer, *On the problem of distribution in globular star clusters*, MNRAS **71**, 460 (1911).

[34] S. P. Goodwin and A. P. Whitworth, *The dynamical evolution of fractal star clusters: The survival of substructure*, A&A **413**, 929 (2004), doi:10.1051/0004-6361:20031529, astro-ph/0310333.

[35] D. C. Heggie, *Binary evolution in stellar dynamics*, MNRAS **173**, 729 (1975).

[36] P. Kroupa, *The Initial Mass Function of Stars: Evidence for Uniformity in Variable Systems*, Science **295**, 82 (2002), doi:10.1126/science.1067524, arXiv:astro-ph/0201098.

[37] T. Sumi, N. Koshimoto, D. P. Bennett, N. J. Rattenbury, F. Abe, R. Barry, A. Bhattacharya, I. A. Bond, H. Fujii, A. Fukui, R. Hamada, Y. Hirao *et al.*, *Free-floating Planet Mass Function from MOA-II 9 yr Survey toward the Galactic Bulge*, AJ **166**(3), 108 (2023), doi:10.3847/1538-3881/ace688, 2303.08280.

[38] H. von Zeipel, *Sur l'application des séries de M. Lindstedt à l'étude du mouvement des comètes périodiques*, Astronomische Nachrichten **183**(22), 345 (1910), doi:10.1002/asna.19091832202.

[39] M. Lidov, Planet. Space Sci. **9**, 719 (1962).

[40] Y. Kozai, *Secular perturbations of asteroids with high inclination and eccentricity*, AJ **67**, 591 (1962).

[41] S. F. Portegies Zwart, T. C. N. Boekholt, E. H. Por, A. S. Hamers and S. L. W. McMillan, *Chaos in self-gravitating many-body systems. Lyapunov time dependence of N and the influence of general relativity*, A&A **659**, A86 (2022), doi:10.1051/0004-6361/202141789, 2109.11012.

[42] S. Portegies Zwart, S. L. W. McMillan, E. van Elteren, I. Pelupessy and N. de Vries, *Multi-physics simulations using a hierarchical interchangeable software interface*, Computer Physics Communications **183**, 456 (2013), doi:http://dx.doi.org/10.1016/j.cpc.2012.09.024, 1204.5522.

[43] F. I. Pelupessy, A. van Elteren, N. de Vries, S. L. W. McMillan, N. Drost and S. F. Portegies Zwart, *The Astrophysical Multipurpose Software Environment*, A&A **557**, A84 (2013), doi:10.1051/0004-6361/201321252, 1307.3016.

[44] S. Portegies Zwart and S. McMillan, *Astrophysical Recipes; The art of AMUSE*, doi:10.1088/978-0-7503-1320-9 (2018).

[45] S. Portegies Zwart and T. Boekholt, *On the minimal accuracy required for simulating self-gravitating systems by means of direct n-body methods*, The Astrophysical Journal Letters **785**(1), L3 (2014).

[46] A. Blaauw, *On the origin of the O- and B-type stars with high velocities (the "run-away" stars), and some related problems*, Bul. Astron. Inst. Neth. **15**, 265 (1961).

[47] S. M. Vicente and J. Alves, *Size distribution of circumstellar disks in the Trapezium cluster*, A&A **441**, 195 (2005), doi:10.1051/0004-6361:20053540, astro-ph/0506585.

[48] S. J. Aarseth and D. C. Heggie, *The probability of binary formation by three-body encounters*, A&A **53**, 259 (1976).

[49] N. Moeckel and C. J. Clarke, *The formation of permanent soft binaries in dispersing clusters*, MNRAS **415**(2), 1179 (2011), doi:10.1111/j.1365-2966.2011.18731.x, 1103.2306.

[50] S. F. Portegies Zwart and S. L. W. McMillan, *Gravitational thermodynamics and black-hole mergers*, Int, J, of Mod. Phys, A **15**, 4871 (2000), doi:10.1142/S0217751X00002135.

[51] G. Van Rossum and F. L. Drake, *Python 3 Reference Manual*, CreateSpace, Scotts Valley, CA, ISBN 1441412697 (2009).

[52] T. E. Oliphant, *A guide to NumPy*, vol. 1, Trelgol Publishing USA (2006).

[53] P. Virtanen, R. Gommers, T. E. Oliphant, M. Haberland, T. Reddy, D. Cournapeau, E. Burovski, P. Peterson, W. Weckesser, J. Bright, S. J. van der Walt, M. Brett *et al.*, *SciPy 1.0: Fundamental Algorithms for Scientific Computing in Python*, Nature Methods **17**, 261 (2020), doi:10.1038/s41592-019-0686-2.

[54] J. D. Hunter, *Matplotlib: A 2D Graphics Environment*, Computing in Science and Engineering **9**, 90 (2007), doi:10.1109/MCSE.2007.55.

[55] S. Portegies Zwart, *The ecological impact of high-performance computing in astrophysics*, Nature Astronomy **4**, 819 (2020), doi:10.1038/s41550-020-1208-y, 2009.11295.

[56] M. Wittmann, G. Hager, T. Zeiser, J. Treibig and G. Wellein, *Chip-level and multi-node analysis of energy-optimized lattice boltzmann cfd simulations*, Concurrency and Computation: Practice and Experience **28**(7), 2295 (2016), doi:10.1002/cpe.3489, https://onlinelibrary.wiley.com/doi/pdf/10.1002/cpe.3489.

A Similarity between r_{ij} and a

The comparison between simulations and observations is somewhat hindered by the different perspecitves. Whereas dynamicists prefer to use Kepler orbital elements, from an observational perspective such data is not always available. In our current study, we try to compare populations of binaries with observed objects. The latter are projected separations, which do not directly translate in orbital elements without full knowledge of the 6-dimension phase space of the orbit. We therefore have to compare projected separation with what we prefer to use, the semi-major axis of a bound two body orbit.

Figures 17 and 18 motivate our choice of analysing results in terms of the semi-major axis given the similarity between the curves. In all cases, r_{ij} exhibits longer tails at shorter separations/orbits. However, these differences are so small, especially in the fractal case, and considering the width of the distribution (illustrated with the large values for the quartile intervals) we can safely interchange between one and the other. In doing so, we assume that the observed projected separation of JuMBOs are equivalent to their semi-major axis, easing our discussion.

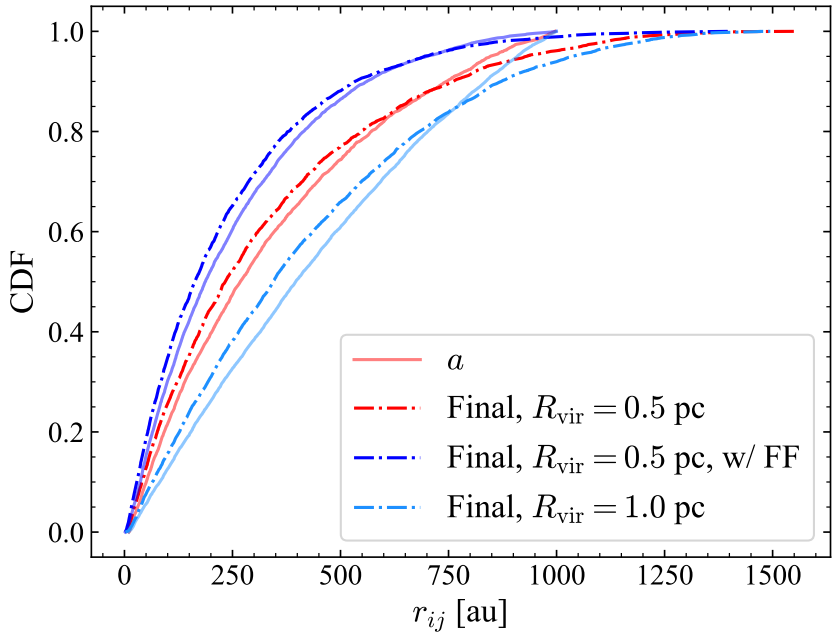

Figure 17: CDF of surviving JuMBO projected separation distribution for models P05, P05FF, P1. Overplotted are translucent lines denoting the respective models' JuMBOs semi-major axis.

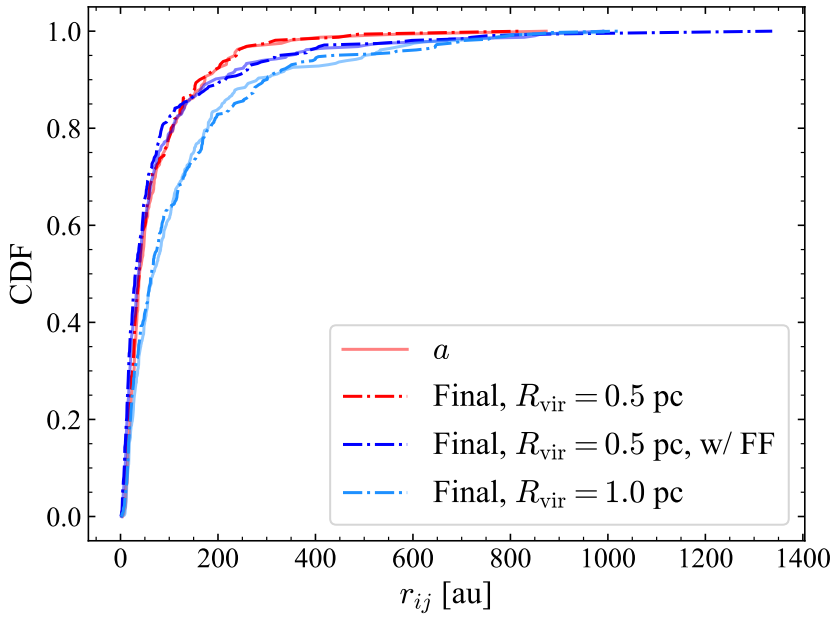

Figure 18: CDF of surviving JuMBO projected separation distribution for models F05, F05FF, F1. Overplotted are translucent lines denoting the respective models' JuMBOs semi-major axis. **ERWAN: could this, and the previous figure, have the same x-axis range?**